RNI: DELENG/2005/15153
Publication: 23rd of every month
Posting: 27th/28th of every month at DPSO

No: DL(E)-01/5079/2023-25
Licensed to post without pre-payment U(E) 28/2023-25
Rs.150

ISSN 0973-2136

www.mycoordinates.org

Coordinates

Volume XXI, Issue 10, October 2025

THE MONTHLY MAGAZINE ON POSITIONING, NAVIGATION AND BEYOND

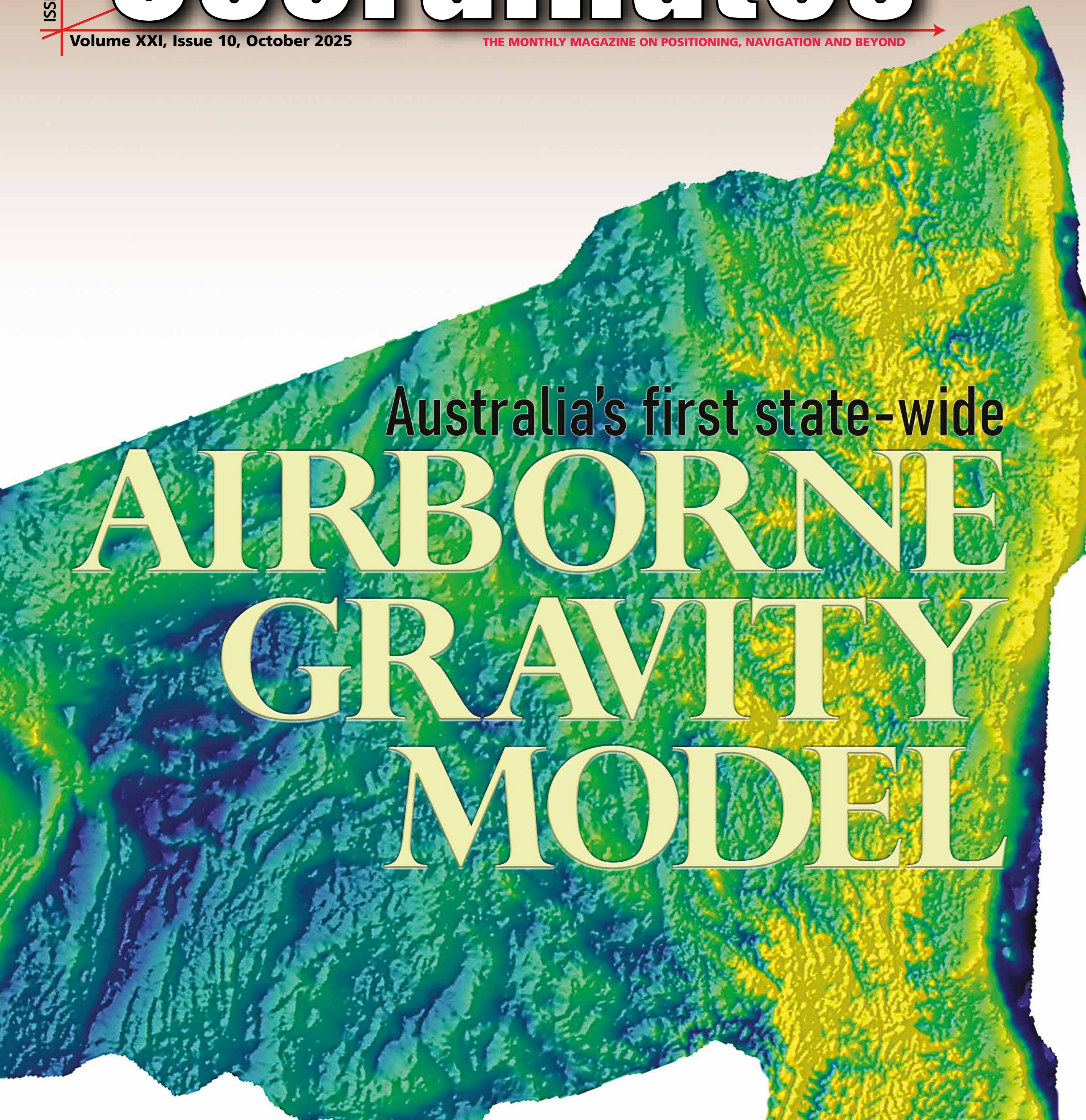

Australia's first state-wide AIRBORNE GRAVITY MODEL

Landslide Vulnerability Mapping for Himachal Pradesh

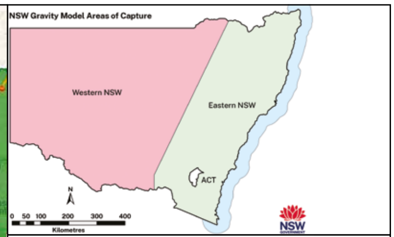

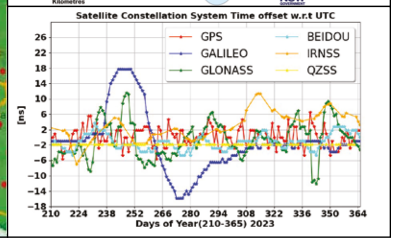

In this issue

Coordinates Volume 21, Issue 10, October 2025

Articles

Columns

This issue has been made possible by the support and good wishes of the following individuals and companies
Maria Jansen, Narayan Dhital, Satish Kumar Negi, Shashi Shekhar, Thomas Grinter
and; Volker Janssen, Riegl, SBG System, and many others.

Mailing Address
A 002, Mansara Apartments
C 9, Vasundhara Enclave
Delhi 110 096, India.
Phones +91 11 42153861, 98102 33422, 98107 24567

Email
[information] talktous@mycoordinates.org
[editorial] bal@mycoordinates.org
[advertising] sam@mycoordinates.org
[subscriptions] iwant@mycoordinates.org
Web www.mycoordinates.org

Annual subscription (12 issues)
[India] Rs.1,800* [Overseas] US$100*
*Excluding postage and handling charges

Printed and published by Sanjay Malaviya on behalf of Coordinates Media Pvt Ltd
Published at A 002 Mansara Apartments, Vasundhara Enclave, Delhi 110096, India.
Printed at Thomson Press (India) Ltd, Mathura Road, Faridabad, India

Editor Bal Krishna
Owner Coordinates Media Pvt Ltd (CMPL)

This issue of Coordinates is of 36 pages, including cover.

Not about if, but when

The *Global Tipping Points Report 2025*,
Prepared by the Global Systems Institute at the University of Exeter,
With the participation of 160 scientists,
Warns that Earth has crossed its first climate tipping point.

Coral reefs, once radiant ecosystems,
Are collapsing under relentless ocean heat.

Their bleaching is not just a marine tragedy,
It's the planet's early warning.

As reefs die, food chains fracture,
Coastlines weaken, and economies tremble.

Greater dangers wait ahead,
The Amazon, the polar ice sheets, the Atlantic currents,
All showing signs of strain.

It is no longer a question of *if*, but *when*.

The scenario hints at catastrophic consequences,
And demands urgent policy responses,
That will define,
And decide the future of our planet.

Bal Krishna, Editor
bal@mycoordinates.org

Australia's first state-wide airborne gravity model

This paper presents some background on airborne gravimetry, introduces the NSW Gravity Model and outlines the benefits it will provide to the surveying profession and wider community.

Dr Volker Janssen
Geodetic Surveyor in the Geodesy & State Adjustment team at DCS Spatial Services, NSW Department of Customer Service, in Bathurst, Australia.

Thomas Grinter
Surveyor-General and Director of Survey at DCS Spatial Services, NSW Department of Customer Service, in Bathurst, Australia.

Maria Jansen
Senior Project Officer in the Project Management Office at DCS Spatial Services, NSW Department of Customer Service, in Bathurst, Australia.

Gravity is not only a fundamental force in physics, surveying and geodesy but also crucial for life in general. It pins our atmosphere to the Earth, keeps our feet on the ground and causes fluids to flow downhill. Today's modern Australian surveyor regularly works with two types of heights: ellipsoidal heights referred to the Geocentric Datum of Australia 2020 (GDA2020, see Harrison et al., 2024) and physical heights referred to the Australian Height Datum (AHD), Australia's first and only legal vertical datum (Janssen and McElroy, 2021). A new third option, the Australian Vertical Working Surface (AVWS), offers an alternative for early adopters and/or precise users requiring higher-quality physical heights (current accuracy about 4-8 cm) than those AHD can provide (accuracy about 6-13 cm) (ICSM, 2021). Global Navigation Satellite System (GNSS) users can access AVWS by applying the Australian Gravimetric Quasigeoid (AGQG, see Featherstone et al., 2018) model to their GDA2020 ellipsoidal heights, just like AUSGeoid2020 is used to obtain AHD heights (Featherstone et al., 2019).

Both geoid models can be improved by collecting high-quality, consistent and evenly distributed gravity measurements to complement and update the existing geoscientific datasets, which are mostly based on regional-scale, historical precompetitive datasets and modern targeted data capture for mineral resource exploration (consisting of a combination of land-based and airborne gravity data collected over several decades). This improvement is best achieved via airborne gravity measurements. A big advantage of gravity data is that it (generally) does not change over time, so it can be captured once and used many times for many diverse applications, provided it is available at sufficient quality and density.

Of particular interest to surveyors in New South Wales (NSW) is that DCS Spatial Services, a unit of the NSW Department of Customer Service (DCS), hosts the largest state-owned and operated GNSS Continuously Operating Reference Station (CORS) network in Australia (Janssen et al., 2016). To unlock the full potential of CORSnet-NSW, a state-wide gravity model is required to improve both geoid models and deliver consistent, higher-quality heighting across the state.

This paper introduces the NSW Gravity Model, the nation's first state-wide gravity model produced from a survey captured in a single airborne campaign, which was delivered by DCS Spatial Services in collaboration with the Geological Survey of NSW and Geoscience Australia (Janssen et al., 2025). It presents some background on airborne gravimetry, discusses data collection and processing, and outlines the benefits this model will provide to the surveying profession and wider community, with gravity data made freely available to the public for the benefit of all.

Airborne gravimetry

Gravity is the force acting on a body on or near the Earth's surface, which is a combination of the gravitational force (the force of attraction between two masses) and the centrifugal force (the apparent force caused by the uniform circular motion of a body about a fixed point) of the Earth's rotation. In the absence of friction and other forces, it is the rate at which objects will accelerate towards each other. At the Earth's surface, gravity (acceleration) is approximately 9.8 m/s^2, with absolute gravitational acceleration varying across Australia between 9.780 m/s^2 in northern Australia and 9.805 m/s^2 in southernmost Tasmania (Kennett et al., 2018).

In principle, gravity can be measured using an accelerometer, which houses a proof mass that is restricted to movement along a sensitive axis and a restraining device (e.g. a spring). The mass is supported by the restraining device and displaces with respect to an equilibrium position when subject to acceleration. Knowing the relationship between the displacement and the restoring force applied to the mass (e.g. due to Hooke's law), the accelerometer provides a measure of the force required to counter the force due to accelerations acting on the mass. Gravity is generally measured in units of gal (1 Gal = 1 cm/s^2) or milligal (mGal).

An absolute gravity meter (or gravimeter) measures gravity at a single location, which is currently restricted to ground-based acquisition. It determines the actual value of the gravitational acceleration, generally by measuring the speed of a falling mass in vacuum using a laser beam and optical interferometry. A relative gravimeter is much more common and measures the difference in gravity between two locations via ground-based, shipborne, airborne or satellite-based acquisition, generally using a spring supporting a proof mass. To be truly effective, this must include acquisition at one or more sites where absolute gravity is known (e.g. an existing gravity mark at the airport where the aircraft is based). Today's airborne gravimetry systems can be separated into traditional airborne gravity systems and gradiometer systems. Both are very complex, requiring a multitude of sophisticated corrections and filtering to extract the desired gravity signal from the measured values.

Airborne gravity systems measure the sum of the aircraft accelerations and the Earth's gravitational field. In simple terms, subtracting the GNSS-derived vertical accelerations of the aircraft from the total vertical gravity measured by the instrument will provide residual gravity. In practice, additional corrections are required to account for platform misalignment (tilt), lever arm (spatial relationship between the GNSS antenna, airborne gravimeter and any other equipment used within the aircraft), horizontal accelerations, drift, Eötvös effect (relative change of the centrifugal force of the Earth's rotation due to being on a moving platform) and minor temperature and pressure variations (Wooldridge, 2010).

The reduction of airborne gravity data requires the use of low-pass filters because the long- to medium-wavelength signal is of interest, while most noise has a short wavelength (i.e. high frequency) and corresponds to limitations in removing inertial accelerations of the aircraft using band-limited GNSS data. Factors influencing resolution and accuracy include aircraft speed, altitude and the spacing of flight lines. While precision from airborne data can be assessed well (using repeat tracks, adjacent tracks, tie lines or crossovers, and grid comparisons), accuracy is much harder to determine (using models, satellite data or ground data) because the true value is not really known, although good global models exist (Preaux, 2016).

Airborne gravity gradiometer systems measure the gradient of the Earth's gravitational field independent of aircraft accelerations. They utilise spinning discs equipped with multiple accelerometers, which measure two or more components of the gravity gradient tensor depending on the number of discs and their orientation. The discs rotate which makes the gravity signal periodic of short temporal baselines, so that the gravity signal can be separated from drift in the accelerometers. The gradients measured at different locations are then transformed to vertical gravity. Gravity gradients are measured in units of Eötvös (Eö), where 1 Eö = 10^{-9}/s^2 = 0.1 mGal/km, i.e. a variation of 1 mGal/km is 10 Eö (Fairhead et al., 2017).

Airborne gravity gradiometer systems are generally more accurate (higher resolution) and more robust because they are less sensitive to aircraft accelerations, but also much more expensive. They must detect very small differential gravitation signals over a short baseline.

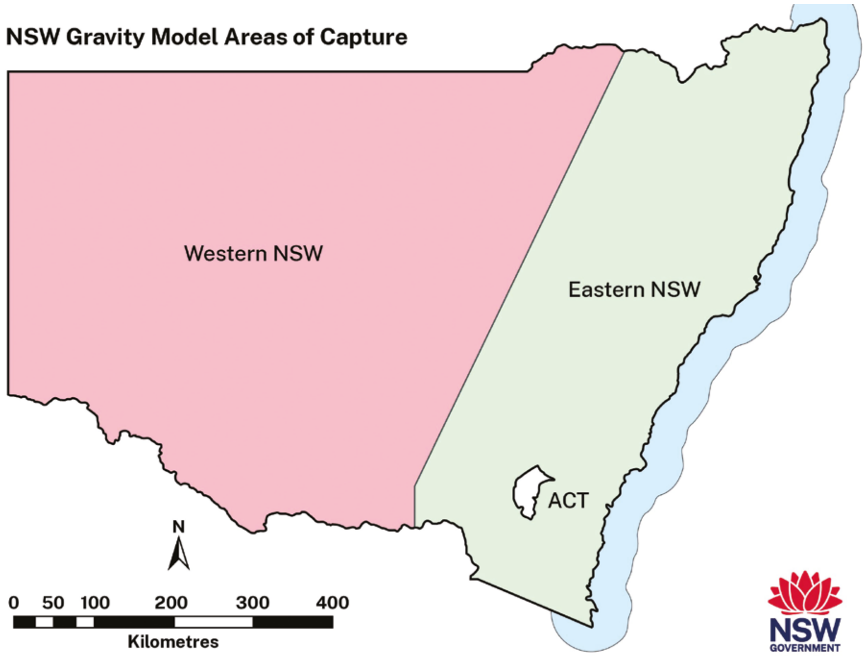

Figure 1: Area of gravity data capture across NSW, divided into an eastern and western part.

Figure 2: Refuelling operations of both Sander Geophysics survey aircraft at Mallacoota Airport, Victoria (Sander Geophysics, 2024).

This requires accounting for scale factor errors and accelerometer bias drift (accelerometers are not perfectly matched), alignment errors (sensitive axes of the accelerometers are not parallel), asymmetry of the configuration (measurement point is not the centre of mass of the accelerometer pair) and self-gradients (the gradient field is changed due to the rotation of the aircraft about the stabilised platform hosting the instrument), which is mostly achieved through calibration and filtering (Jekeli, 2003).

Data collection & processing

NSW is a large state (about 1.5 times the size of France) encompassing an area of 800,000 km^2 and a coastline of 2,100 km in length, with terrain varying from vast plains to rugged mountainous areas (elevations up to 2,228 m at Mt Kosciuszko). In order to facilitate efficient data collection utilising two expert contractors, the area of interest (which also includes the offshore area up to 50 km from the east coast) was divided into two parts: Eastern NSW and Western NSW (Figure 1). These two parts (each completed by a single contractor) were then stitched together to produce the final products. The total area of capture amounted to 820,000 km^2, also covering another jurisdiction, the Australian Capital Territory (ACT), in its entirety.

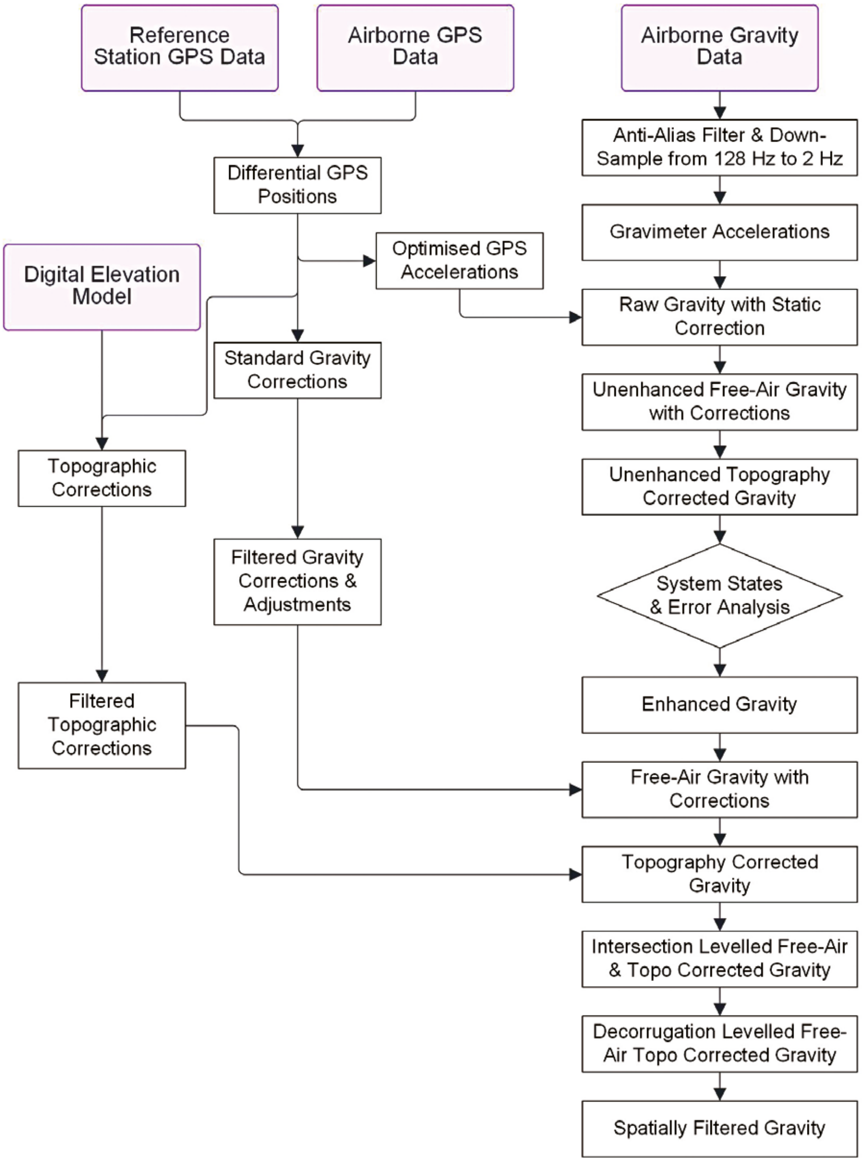

Figure 3: Gravity data processing flowchart (adapted from Sander Geophysics, 2024).

Eastern NSW

Sander Geophysics was contracted to complete Eastern NSW (Sander Geophysics, 2024). This area covers slightly more than the eastern third of NSW, including the Great Dividing Range, the ACT and the offshore margin up to 50 km from the coast (which includes the continental shelf). In the west, it is bordered roughly by a line through the towns of Narrabri, Dubbo and Wagga Wagga.

The principal survey traverse lines were oriented at 20º clockwise from north and spaced at 2,250 m onshore and 2,500 m offshore. A selected area of denser infill lines (mainly covering the north-east of NSW) resulted in lines spaced 1,125 m onshore and 1,250 m offshore. Tie lines for crossover checking used to level the survey data were oriented east-west at 90º and spaced at 75 km. A drape surface used to guide the aircraft's height above the ground was created, considering the terrain and the performance of the aircraft at the expected altitudes and estimated temperatures. The survey was flown with a target clearance of 160 m above ground level, following the drape. Due to air traffic control restrictions, the area around Sydney Airport was flown at higher altitudes (between 518 m and 610 m). The target average ground speed was 60 m/s.

Due to safety and environmental considerations, the survey was split into 'hostile' and 'non-hostile' areas. The western, non-hostile area was flown with a single-engine Cessna C208B Grand Caravan, while the eastern 'hostile' area (i.e. densely populated and offshore areas) was flown using a twin-engine de Havilland DHC-6 Twin Otter (Figure 2). Bases of operation were Orange, Cessnock, Tamworth and Kempsey, as well as Mallacoota, Victoria.

Production flights commenced in August 2022 and lasted for 16 months, with data acquisition spanning all four seasons. Summer weather was usually hot and dry but occasionally interrupted by wet spells with significant rainfall. In autumn, winter and spring, higher elevations experienced long periods of wet weather with low visibility, causing many days when survey flights were not possible. On a few occasions, large parts of the survey area were subject to heavy rains and flooding. A total of 242 flights were carried out to complete the planned 223,318 line kilometres.

The position of the temporary GNSS reference stations at each airport was calculated via Precise Point Positioning (PPP) corrections using the algorithm developed by Natural Resources Canada for its CSRS-PPP online positioning service (NRCan, 2025), which has been incorporated into the suite of software used.

Gravity data was collected with the Airborne Inertially Referenced Gravimeter (AIRGrav) system, which was designed by Sander Geophysics specifically for the unique characteristics of the airborne environment. The relative airborne data was tied to absolute gravity by connecting to a nearby Australian Fundamental Gravity Network (AFGN) station, typically already established at the airport. The gravimeter was then calibrated at the aircraft's exact parking location daily to the local gravity value.

Repeat test lines, planned and established in consultation with DCS Spatial Services, were flown periodically during the data acquisition to demonstrate the accuracy, repeatability and resolution of the AIRGrav system. The location of these 40-50 km long test lines was selected to be operationally efficient to fly from the various airports, covered by pre-existing Geoscience Australia gravity data grids and sufficiently removed from significant settlements or installations.

Sander Geophysics' proprietary software was used for data processing, which involved numerous corrections and filtering of the observed gravity data. A simplified processing flowchart is shown in Figure 3, illustrating the complexity of the procedure. The airborne GNSS antenna location was determined with an accuracy of better than 5 cm by differentially correcting the airborne GNSS data with respect to the reference stations.

The raw gravity data was corrected for the effects of aircraft acceleration before the standard corrections were applied, i.e. Eötvös correction, normal gravity correction, atmospheric correction, free-air correction, full 3D topographic Bouguer correction, static correction (absolute gravity was established where the static readings were made before and after the flights so that the relative gravity data could be tied into the national gravity datum) and level correction (based on intersections with tie lines and grid-based de-corrugation). Tidal corrections were not applied, as they are generally not necessary for airborne gravity processing due to their small magnitude. This resulted in determining the free-air anomaly and the Bouguer anomaly (both in mGal).

Simply put, the gravity anomaly indicates the difference of a gravity measurement from the expected value. Depending on the type of correction applied to the observed gravity data at the point of observation, we distinguish between the free-air anomaly (corrected for the height at which it was measured, i.e. reduced to the ellipsoid or geoid) and the Bouguer anomaly (corrected for the height at which it was measured and also the attraction of terrain, i.e. the mass of rock between the measurement point and the ellipsoid or geoid). These anomalies basically show the gravity variation due to the Earth not being quite an ellipsoid/geoid in shape and having variations in density due to the different minerals of which it is made. The free-air gravity anomaly includes all these variations in the shape of the Earth and in the density of the minerals. The Bouguer gravity anomaly removes the signal due to the shape variations and keeps only that due to the density variations, which is most useful for geology and exploration.

Further filtering and gridding followed to reduce noise and generate grids with a 500 m grid size. Firstly, a 70-second, along-track, cosine-tapered low-pass filter (equivalent to a 4,200 m filter when accounting for the aircraft's ground speed of 60 m/s) was selected, and the filtered data was then gridded using a minimum-curvature algorithm that averages all values within any given grid cell and interpolates the data between survey lines to produce a smooth grid. In the second filtering stage, low-pass filtering (directly equivalent to spatial averaging) was applied to the grid to achieve better noise reduction than by simply increasing the degree of line filtering. Essentially, the survey area is over-sampled by a line spacing that is smaller than the grid filter used. The low-pass filter acts to average data within the radius of its filter dimension, retaining the common signal on adjacent lines and cancelling out random noise. The final data provided a resolution of 2,100 m and 2,500 m, which is expected for the line spacing used (2,250 m onshore and 2,500 m offshore).

Western NSW

Xcalibur Multiphysics was contracted to complete Western NSW, roughly covering the western two thirds of the state (Xcalibur Multiphysics, 2024). The principal survey traverse lines were oriented due north and spaced at 2,000 m, while tie lines were oriented east-west at 90º and spaced at 73 km. The survey was flown with a target clearance of 160 m above ground level (following a drape) and a target average ground speed of 65 m/s. Flights commenced in June 2022 and lasted for 14 months, with a total of 413 flights conducted to complete 268,517 line kilometres.

A single-engine Cessna C208B Grand Caravan was used, operating out of Broken Hill, Cobar, Dubbo and Griffith, as well as Yarrawonga, Victoria. Temporary GNSS reference stations were established at each airport and coordinated via Geoscience Australia's AUSPOS service (GA, 2025), based on datasets of at least 8 hours duration covering the expected time period of an average production flight.

Gravity data was collected with a Falcon Airborne Gravity Gradiometer (AGG) system, which has been optimised for airborne broadband geophysical exploration. The main steps in the Falcon processing flow utilising Xcalibur proprietary software included a dynamic correction (to reduce the effects of aircraft accelerations), demodulation (to transform the accelerometer measurements in the gravimeter from the rotating frame back into a spatial reference frame), self-gradient correction (to account for time-varying gravity gradients caused by the changing heading and attitude of the aircraft during flight), terrain correction (derived from a Digital Terrain Model and using the standard average crustal density of 2.67 g/cm^3) and level correction to the regional data using the 2019 Australian National Gravity Grid (ANGG, see Lane et al., 2020).

Once the gradient data channels were fully processed and levelled, noise reduction processing was carried out. The quality (precision) of the Falcon data is measured using the Falcon Difference Noise (the two independent sets of gradiometers inside the instrument allow a noise estimate to be taken at each measurement). The data is acceptable if the noise value is below 5 Eö. However, in this case, for lines where the turbulence was greater than 0.981 m/s^2, the noise limit was increased to 7 Eö.

The noise reduction process is designed to reduce acquisition-related noise by targeting signal response with a linear spatial frequency along the survey line direction. This maximises the resolution of the finished dataset so that it is approximately equal to the line spacing, while also reducing the noise power on the measured data. When the line spacing is smaller than the resolution of the initial signal processing, this process allows for a reduction in noise and increase in resolution. In this case, the line spacing was much larger than the initial signal processing resolution, causing a smaller noise reduction effect but still improving final data quality.

Now that the measured gradients were fully processed, the data was transformed into the components of the gradient tensor. This process uses a Fourier transformation approach to transform the measured tensor components into the full gravity gradient tensor data and the vertical gravity data (Dransfield and Chen, 2019).

The final processing step was the regional conforming process, which corrects the vertical gravity data for very long wavelength errors introduced by the vertical integration of the vertical gravity gradient data. The data was conformed via the Earth Gravitational Model 2008 (EGM2008, see Pavlis et al., 2012), using a filter cut-off wavelength of 200 km, followed by terrain corrections using the standard average crustal density of 2.67 g/cm^3.

The conforming process required a significant number of iterations to get an acceptable result as it had never been applied to a survey of such large dimensions before. The standard method had to be revised to ensure the final product met all survey requirements. The approach used was to conform the vertical gravity gradient before the integration. Once this was completed, a second conforming was required to account for very long wavelength integration errors, following the standard methodology but utilising a filter cut-off of 500 km. Considering the line spacing (2,000 m) and the grid size (500 m), the resolution of the final data was determined to be either 1,500 m or 2,000 m.

Quality assurance & final grid production

During and after data acquisition, an independent, third-party subject matter expert checked and verified that the collected data met the quality specifications. Final quality assurance was then performed and the final gridded data products produced (McCubbine, 2024). This ensured that these datasets, captured by two suppliers using different methodologies and equipment, could be integrated into a consistent and reliable set of gravity anomaly grids covering the entire state.

The datasets were evaluated by comparing the point-located and gridded gravity anomaly data to two key reference datasets: the EGM2008 gravity model and the 2019 ANGG. For Eastern NSW, the overall standard deviation of the differences was approximately 2-3 mGal for the comparisons between supplied/recomputed Bouguer anomalies and the ANGG and around 6-7 mGal for the comparison between the geodetic free-air anomaly data and the EGM2008. The Western NSW data also showed high fidelity, with the final gridded datasets exhibiting standard deviations of 1.5 and 1.7 mGal when compared to the ANGG and EGM2008 reference grids, respectively. The higher agreement is due to the Western NSW data undergoing a regional conforming process. These statistics underscore the reliability of the processed datasets for use in regional-scale mapping.

Additional processing was required to ensure consistency across the two datasets. This involved producing a line-by-line levelling adjustment of the Eastern NSW data to align it with an existing state-wide dataset, sampled from the ANGG. This corrected any discrepancies and biases that arose from limitations of the data collection and ensured that the final gridded products accurately reflect the gravity anomalies across NSW. A new point-located data file was reproduced to include the additional levelling corrections and application to the supplied gravity anomalies.

The final data augmentation and gridding process involved the following four steps:

1. Data preparation: The point-located data from both suppliers was extracted and block-averaged to half the flight line spacing on a line-by-line basis.
2. Residual calculation: A long-wavelength reference signal was subtracted from the gravity anomalies to create a 'zero-mean' residual for gridding. The reference signal was derived from a 50 km filtered version of the ANGG data.

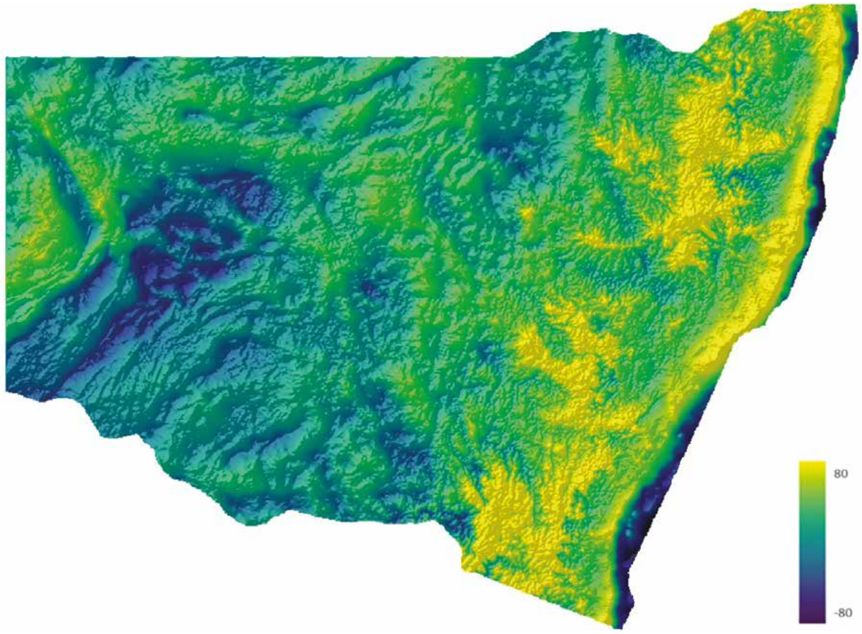

Figure 4: Final gridded free-air gravity anomaly at flight elevation in mGal (McCubbine, 2024).

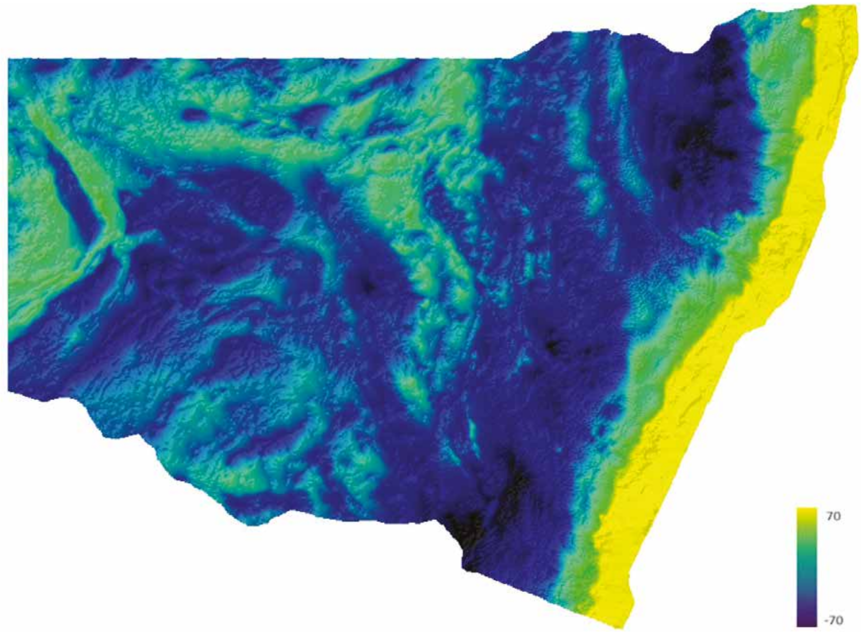

Figure 5: Final gridded Bouguer gravity anomaly at surface level in mGal (McCubbine, 2024).

3. Gridding: The residuals were interpolated using Least Squares Collocation (LSC), a method that accounts for spatial correlations in the data. This involved fitting the Forsberg (1987) covariance function and solving matrix inversion problems to produce gridded datasets at a 15 arc-second resolution.
4. Restoring long wavelengths: The reference signal was added back to the gridded residuals to produce the final gravity anomaly grids.

Three final gridded datasets were produced in the GDA2020 at a resolution of 15 arc-seconds (500 m):

- Free-air gravity anomaly at flight elevation (Figure 4).
- Bouguer gravity anomaly at flight elevation.
- Bouguer gravity anomaly downward continued to the topographic surface (Figure 5).

Two surfaces were established as grid nodes to facilitate the interpolation of gravity anomaly data onto a regular grid. The first, a 'flight-level surface', was derived by block-averaging the aircraft's GNSS positioning data into 500 m grid cells, representing the flight elevation grid nodes. The second, a 'topographic surface', was constructed by clipping out the relevant area from the 2019 ANGG ellipsoidal Digital Elevation Model, providing a surface-level height reference. The point-located gravity anomaly data was then interpolated onto a 15 arc-second output grid using LSC, ensuring consistency between the reference surfaces and the final gridded product. These gridded gravity datasets provide seamless, coherent maps of the gravity field across NSW. The careful assessment, correction and gridding processes have ensured that these datasets are accurate, reliable and suitable for a wide range of applications.

A state-wide gravity model for NSW

The NSW Gravity Model was delivered on time and within scope and budget due to a collaborative approach between DCS Spatial Services, the Geological Survey of NSW and Geoscience Australia. The collective commitment to enhance the quality of the gravity model by uniting our efforts across state and federal government departments was a strategic decision made to make NSW an easier and more productive place to work, while also supporting national interests. Working closely with experts across different teams allowed us to maximise the collective impact for many diverse applications, delivering the best possible benefit for our customers. As a by-product, we even delivered a gravity model for the ACT, an entirely different jurisdiction – this was much easier than flying around it!

DCS Spatial Services was responsible for managing the project, with Geoscience Australia providing technical expertise and the Geological Survey of NSW ensuring that the project specifications met the requirements to deliver a fair playing field for exploration. Gravity datasets are very useful for geodesy and geology, but these two sciences have slightly different requirements. The former needs gravity relative to the geoid, while the latter needs gravity relative to the ellipsoid. Close collaboration ensured that these requirements were met, along with supporting other use cases.

The general public was informed and educated about the data collection flights by DCS Spatial Services via media releases, Frequently Asked Questions and its website (including a video detailing the work to be undertaken). It was stressed that people's privacy would be protected as the aircraft would only be equipped with an instrument measuring gravity data and not be capable of capturing images of property, infrastructure or individuals. It was also emphasised that these instruments do not emit any signals or impact people, animals or infrastructure and have been used for decades throughout Australia and globally.

Challenges encountered and resolved along the way included delays due to adverse weather conditions or scheduled aircraft maintenance, landholder complaints across Western NSW, access to restricted airspaces, AGG sensor system failure, twin-engine aircraft availability for data acquisition, unaccounted safety audits due to the use of multiple aircraft, optimistic time allocation for data processing, issues related to meeting the contract specifications, and difficulties in the integration and merging of the datasets collected by the two suppliers.

We gratefully acknowledge the collaboration with other state jurisdictions undertaking airborne gravity surveys at the time, which was crucial in enabling the NSW data capture to be completed on time. In particular, Land Use Victoria, the Geological Survey of Victoria and the South Australian government are thanked for providing access to the twin-engine aircraft being used for their gravity surveys.

Data availability & benefits

The gravity data is owned by the NSW Government and freely available to the public via its Spatial Collaboration Portal (DCS Spatial Services, 2025) and the Geological Survey of NSW's MinView platform (DPIRD, 2025). It is also included in the national geoscience database and accessible via the Geophysical Archive Data Delivery System (GADDS) managed by Geoscience Australia. Making data available in various forms enables it to be used and combined with other sources to generate valuable products for diverse applications. Derived products, such as updated geoid models for GNSS positioning, will be made available in due course.

The NSW Gravity Model positions NSW as a leader in airborne gravity data coverage in Australia. This new dataset will significantly improve the gravity (and gravimetric quasigeoid) model and thus the accuracy of GNSS-derived physical heights for a wide range of applications relying on the flow of fluids, such as floodplain management and flood modelling, waterway navigation management, roadway and drainage design, groundwater management, agricultural management, and surveying in general. It will also allow geoscientists to further their understanding of Australia's geology and how it has evolved over time, and assist in the management of earth resources, infrastructure and natural hazards. Finally, the NSW Gravity Model raises the state to the forefront of potential AVWS early adopters and promotes it as an ideal test area to evaluate any new height datum's performance and user impact.

Conclusion

This paper has presented the NSW Gravity Model, Australia's first state-wide gravity model produced from a single airborne gravity survey campaign. It has provided some background on airborne gravimetry, introduced the NSW Gravity Model, discussed its data collection and processing, and outlined the benefits this model will provide to the surveying profession and wider community, with gravity data made freely available to the public for the benefit of all.

References

DCS Spatial Services (2025) Spatial Collaboration Portal, https://portal.spatial.nsw.gov.au/portal/ (accessed Sep 2025).

DPIRD (2025) MinView, https://www.resources.nsw.gov.au/geological-survey/minview (accessed Sep 2025).

Dransfield M.H. and Chen T. (2019) Heli-borne gravity gradiometry in rugged terrain, *Geophysical Prospecting*, 67(6), 1626-1636.

Fairhead J.D., Cooper G.R.J. and Sander S. (2017) Advances in airborne gravity and magnetics, *Proceedings of Exploration'17: Sixth Decennial International Conference on Mineral Exploration*, Toronto, Canada, 22-25 October, 113-127.

Featherstone W.E., McCubbine J.C., Brown N.J., Claessens S.J., Filmer M.S. and Kirby J.F. (2018) The first Australian gravimetric quasigeoid model with location-specific uncertainty estimates, *Journal of Geodesy*, 92(2), 149-168.

Featherstone W.E., McCubbine J.C., Claessens S.J., Belton D. and Brown N.J. (2019) Using AUSGeoid2020 and its error grids in surveying computations, *Journal of Spatial Science*, 64(3), 363-380.

Forsberg R. (1987) A new covariance model for inertial gravimetry and gradiometry, *Journal of Geophysical Research*, 92(B2), 1305-1310.

GA (2025) AUSPOS – Online GPS processing service, http://www.ga.gov.au/scientific-topics/positioning-navigation/geodesy/auspos (accessed Sep 2025).

Harrison C., Brown N., Dawson J. and Fraser R. (2024) Geocentric Datum of Australia 2020: The first Australian datum developed from a rigorous continental-scale adjustment, *Journal of Spatial Science*, 69(1), 167-179.

ICSM (2021) Australian Vertical Working Surface (AVWS) technical implementation plan, version 1.6, https://www.icsm.gov.au/publications/australian-vertical-working-surface-technical-implementation-plan-v16 (accessed Sep 2025).

Janssen V., Grinter T. and Jansen M. (2025) The NSW Gravity Model: Australia's first state-wide airborne gravity model, *Proceedings of FIG Working Week 2025*, Brisbane, Australia, 6-10 April, 19pp.

Janssen V., Haasdyk J. and McElroy S. (2016) CORSnet-NSW: A success story, *Proceedings of Association of Public Authority Surveyors Conference (APAS2016)*, Leura, Australia, 4-6 April, 10-28.

Janssen V. and McElroy S. (2021) The Australian Height Datum turns 50: Past, present & future, *Proceedings of APAS Webinar Series 2021 (AWS2021)*, 24 March – 30 June, 3-27.

Jekeli C. (2003) Statistical analysis of moving-base gravimetry and gravity gradiometry, Report no. 466, Geodetic Science, Ohio State University, Columbus, Ohio.

Kennett B.L.N., Chopping R. and Blewett R. (2018) *The Australian continent: A geophysical synthesis*, ANU Press & Geoscience Australia, Canberra, 133pp.

Lane R.J.L., Wynne P.E., Poudjom Djomani Y.H., Stratford W.R., Barretto J.A. and Caratori Tontini F. (2020) 2019 Australian National Gravity Grids explanatory notes, https://ecat.ga.gov.au/geonetwork/srv/eng/catalog.search#/metadata/144233 (accessed Sep 2025).

McCubbine J. (2024) New South Wales statewide gravity anomaly maps from airborne gravimetry data – Processing report: Data assessment, augmentation and grid production, unpublished technical report.

NRCan (2025) CSRS-PPP, https://webapp.geod.nrcan.gc.ca/geod/tools-outils/ppp.php (accessed Sep 2025).

Pavlis N.K., Holmes S.A., Kenyon S.C. and Factor J.K. (2012) The development and evaluation of the Earth Gravitational Model 2008 (EGM2008), *Journal of Geophysical Research: Solid Earth*, 117(B4), B04406.

Preaux S. (2016) Airborne gravity data quality assessment, presented at NGS Airborne Gravity for Geodesy Summer School, Silver Spring, Maryland, 23-27 May, https://www.ngs.noaa.gov/GRAV-D/2016SummerSchool/ (accessed Sep 2025).

Sander Geophysics (2024) Airborne gravity survey in New South Wales, eastern block, unpublished technical report.

Wooldridge A. (2010) Review of modern airborne gravity focusing on results from GT-1A surveys, *First Break*, 28(5), 85-92.

Xcalibur Multiphysics (2024) NSW Live Program: NSW Gravity Model – Processing and logistics report, unpublished technical report.

Landslide Vulnerability Mapping for Himachal Pradesh

We present a detailed landslide vulnerability map developed on the Google Earth Engine (GEE) platform using a Weighted Overlay Model.

Dr. Satish Kumar Negi
Associate Professor, Department of Geography, Govt. Degree College Dharampur, Solan, Himachal Pradesh, India

Shashi Shekhar
Scientific Officer, H.P. State Pollution Control Board, Shimla, Himachal Pradesh, India

Abstract

This study addresses the escalating threat of landslides in Himachal Pradesh, exacerbated by a combination of a fragile Himalayan ecosystem, a heavy monsoon climate, and unplanned human development. The devastating 2025 monsoon season, which resulted in over 360 fatalities and crores in economic losses, underscores the urgent need for effective risk mitigation. We present a detailed landslide vulnerability map developed on the Google Earth Engine (GEE) platform using a Weighted Overlay Model. The methodology integrates nine key parameters, including rainfall intensity, slope, land use change (particularly implemented through forest loss during 2000-2020), and proximity to roads apart from others, with each factor assigned a weight based on its contribution to landslide risk. Our analysis highlights that the mid-hills, where a mix of steep terrain and human settlements exists, are the most vulnerable. Specific high-risk zones were identified in districts such as Kullu, Mandi, Shimla, Chamba and Kinnaur. The resulting map serves as a vital tool for informing policy decisions and enhancing disaster preparedness. The paper concludes by emphasizing the critical need for sustainable development and resilient planning to safeguard Himachal Pradesh's fragile landscape from future catastrophes.

Note: The analysis presented here is the sole responsibility of the authors and does not reflect the views of their respective organizations. The findings are based on secondary data and are intended as an academic exercise.

1. Introduction

Landslides are a pervasive natural hazard in the Himalayan state of Himachal Pradesh, a region characterized by its young geology, tectonic activity, and a heavy monsoon climate. To effectively manage and mitigate the risks posed by these events, it's crucial to identify and map areas of high susceptibility. This paper uses an advanced geospatial approach on the Google Earth Engine (GEE) platform to create a detailed landslide vulnerability map. By combining and analysing multiple environmental and anthropogenic factors, the model produces a comprehensive vulnerability index that can help to make informed policy decisions and disaster preparedness strategies.

2. Landslides in Himachal Pradesh (2025)

Himachal Pradesh has faced one of its most devastating monsoon seasons in recent years, with landslides, flash floods, and cloudbursts wreaking havoc across the hill state. As of early September 2025, the official toll of rain-related disasters has risen to more than 200 deaths, while total fatalities, including those from road accidents triggered by adverse conditions, have crossed 360. Hundreds more have sustained injuries, and thousands of families have been displaced.

Himachal Pradesh has a long history of recurring landslides, occurring almost every monsoon season. One scientific record of these events is the Global Landslide Catalog (GLC), developed by NASA's Goddard Space Flight Center. The

GLC systematically documents rainfall-triggered landslide events worldwide, regardless of their size, location, or impact, drawing on sources such as media reports, disaster databases, scientific studies, and other reliable records. Compiled since 2007 and covering the period from 2007 to 2019, the dataset provides a unique global baseline of landslide occurrences. Analysis of the data demonstrates that a significant number of landslides in Himachal Pradesh occur along major highways and transport corridors, highlighting the vulnerability of critical infrastructure to rainfall-induced hazards.

The destruction to infrastructure and property has been staggering. Official estimates of economic losses range between ₹1,900 crore and over ₹3,000 crore. Entire stretches of road networks have been washed away, leaving hundreds of villages cut off from essential supplies. At the peak of the monsoon fury, close to 300 roads, including national highways, were blocked due to landslides. Power supply was disrupted at several locations, with over 300 transformers damaged, while more than 250 water supply schemes were rendered inoperative.

Private property has also been severely affected. Nearly 4,000 houses have either collapsed or suffered major structural damage, while many more stand partially damaged and unsafe for habitation. Alongside, over 25,000 head of livestock have perished, compounding the economic pain for rural households dependent on agriculture and dairying. Shops, cowsheds, bridges, ghats, and irrigation systems have also been swept away.

The state's water and irrigation infrastructure has been among the worst hit. Out of more than 10,000 water supply and irrigation schemes, around 7,500 suffered damages, leading to losses of over ₹580 crore. While authorities have managed to temporarily restore nearly 95% of drinking water schemes, many remain fragile and vulnerable to further collapse.

Excessive rainfall — nearly 72% above normal in some regions — has intensified the crisis. Cloudbursts and sudden heavy downpours have triggered flash floods, particularly in districts like Kullu, Mandi, Kangra, and Shimla. Tragically, many of the fatalities have occurred at night when landslides buried homes, leaving families with little chance of survival. The Kullu disaster in September, where five members of a single family were killed as their home was destroyed, highlighted the vulnerability of settlements built along unstable slopes.

The impact has not been limited to rural and remote regions. Towns and semi-urban areas have also seen extensive damages, with traffic disruptions, water shortages, and repeated power cuts. Tourism, a vital sector for the state's economy, has also suffered due to the closure of major routes like the Chandigarh-Manali highway.

The widespread damage has underscored the fragility of Himachal Pradesh's ecology in the face of unplanned development and changing rainfall patterns. Experts warn that intense rainfall, coupled with indiscriminate hill cutting, deforestation, and unscientific construction, is steadily increasing the frequency and severity of landslides. The 2025 monsoon season has therefore not only left behind a trail of destruction but also a stark reminder of the urgent need for sustainable development and disaster-resilient planning in the fragile Himalayan ecosystem.

3. Driving cause

Experts have repeatedly warned that the scale of destruction cannot be attributed to rainfall alone. The **driving causes** lie in a dangerous mix of natural fragility and human intervention. The intensity of rainfall has increased sharply in recent years even as its duration has shortened, producing sudden cloudbursts and extreme downpours that the slopes cannot absorb. Compounding this is extensive hill-slope cutting for roads, tunnels, hydropower projects, and unregulated construction across the fragile mountains. Blasting for infrastructure, widespread deforestation, and exploitative land-use practices have

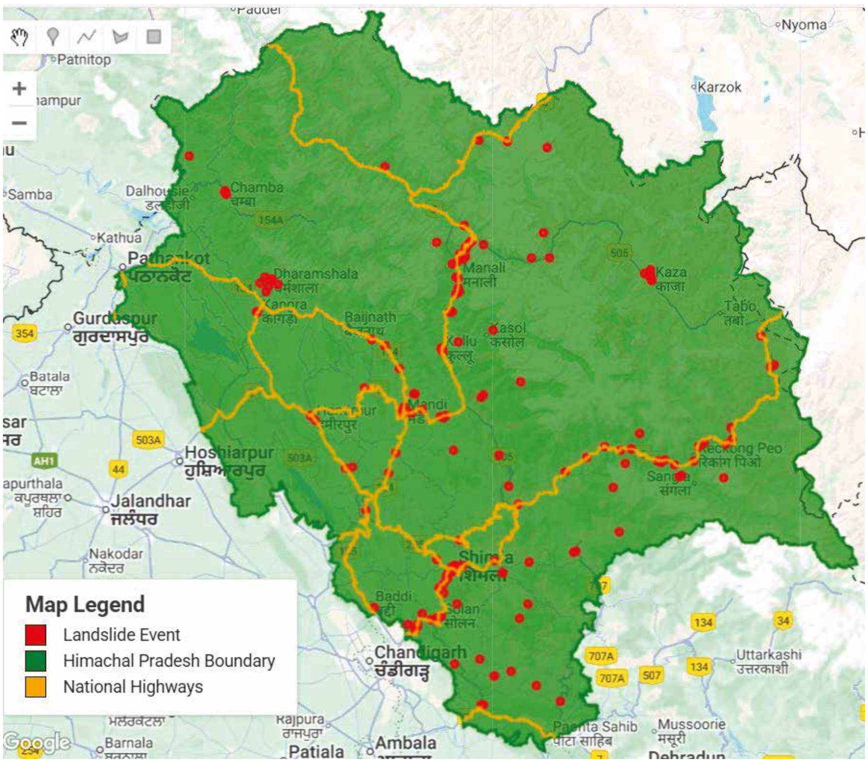

Map-1: Historical landslide events: NASA's Goddard Space Flight Center, the GLC currently covers the period from 2007 to 2019 and represents a unique global dataset, Highways data sources are from secondary sources.

further destabilized the landscape, making it more prone to catastrophic failures during intense rainfall, as highlighted by reports in *The Hindu, Hindustan Times, The Economic Times,* and *India Today*.

4. Hazard Mapping & Regional Vulnerability

Forty-nine per cent of Himachal Pradesh is prone to medium-risk and 40% to high-risk landslides, floods and avalanches, according to a recent study by the Indian Institute of Technology (IIT)- Ropar.

4.1 Geographical risk breakdown:

- **Upper reaches (high altitudes)**: prone to **avalanches**, especially Kinnaur and Lahaul-Spiti.
- **Middle & lower zones**: more vulnerable to **landslides and floods**—notably in Kangra, Kullu, Mandi, Una, Hamirpur, Bilaspur, and Chamba.
- Steeper slopes (16.8°–41.5°) at higher altitude are hotspots for multiple hazards, while moderate slopes (5.9°–16.4°) up to 1,600 m combine flood and landslide susceptibility.

5. Methodology

The core of this project is a **Weighted Overlay Model**, a common technique in geospatial analysis for multi-criteria decision-making. The process involves four main steps:

1. **Parameter Selection**: We identified a set of key factors scientifically known to influence landslides. These included both static (e.g., topography) and dynamic (e.g., rainfall, land use change) variables.
2. **Data Acquisition and Processing**: Using GEE's extensive data catalog, we accessed and processed publicly available datasets. For each factor, we derived a raster layer representing its influence on landslide risk.
3. **Normalization**: To make the layers comparable, each was normalized to a scale from 0 to 1. This step ensures that a factor's original unit of measurement (e.g., meters, degrees) doesn't disproportionately affect the final result.
4. **Weighted Summation**: Each normalized layer was assigned a weight reflecting its relative importance in landslide causation in the Himalayan context. The final vulnerability index for any given location is the sum of all weighted parameters. The formula is as follows:

$$\text{Vulnerability}=\sum_{i=1}^{n}(W_i\times P_i)$$

Where:

- Vulnerability is the final vulnerability score.
- W_i is the assigned weight for parameter i.
- P_i is the normalized value of parameter i.

5. **Weighted Overlay:** This is the central calculation step. The vulnerability image is created by multiplying each normalized layer by a predefined weight and then adding them all together.
6. The weights reflect the relative importance of each factor. For instance, rainfall and slope are given higher weights (0.20 and 0.15) because they are typically major drivers of landslides, while aspect and drainage proximity are given lower weights (0.05).
7. The formula is: Vulnerability = (Slope×0.15)+(Aspect×0.05) +(Curvature×0.05) +(Rainfall×0.20)+(NDVI×0.10) +(LandUseChange×0.15) +(Dist. Roads×0.15)+(TWI×0.15)+(Dist. Drainage×0.05)

6. Parameters and Justification

The following parameters were selected and justified based on their role in slope stability and landslide occurrence.

1. **Slope**: The most fundamental parameter. Steep slopes increase the gravitational force acting on the soil mass, making them inherently more unstable. A higher slope angle directly correlates with increased landslide risk.
   - **Data Source**: USGS SRTM Digital Elevation Model (DEM). This global dataset provides high-resolution elevation data necessary for precise slope calculations.
   - **Justification**: A weight of **0.15** was assigned, recognizing that slope is a primary driver of mass movement.
2. **Rainfall Intensity**: Prolonged or intense rainfall saturates soil and bedrock, increasing pore water pressure and significantly reducing the soil's shear strength. This is a major triggering factor for landslides in the monsoon-dominated climate of Himachal Pradesh.
   - **Data Source**: CHIRPS (Climate Hazards Group InfraRed Precipitation with Station data). This dataset provides long-term daily rainfall averages, capturing the region's precipitation patterns.
   - **Justification**: With a weight of **0.20**, rainfall is considered the most significant contributing factor.
3. **Land Use Change**: Human activities like deforestation, construction, and agricultural expansion alter natural drainage patterns and destabilize slopes by removing vegetation cover.
   - **Data Source**: ESA WorldCover. By comparing the 2020 and 2021 versions of this global land cover dataset, we created a binary layer identifying areas where land use has changed, indicating recent human intervention. Both years provide 10-meter resolution global land cover maps, developed by ESA in collaboration with Wageningen University and supported by Copernicus.
   - **Justification**: A weight of **0.15** reflects the significant role of human activity in triggering landslides.
4. **Proximity to Roads**: Road construction in mountainous terrain often involves slope cutting and excavation, which removes toe support and disrupts the natural stability of the hill.
   - **Data Source**: OpenStreetMap. This dataset provides a detailed road network from which we computed the distance of any given point to the nearest road.

- **Justification**: With a weight of **0.15**, this factor is highly influential, as a vast majority of landslides are triggered by human infrastructure development.

5. **Topographic Wetness Index (TWI)**: TWI is an indicator of soil moisture accumulation. High TWI values point to areas where water naturally converges, making the ground oversaturated and vulnerable to failure.
   - **Data Source**: Derived from the USGS SRTM DEM.
   - **Justification**: A weight of **0.15** was given, as water accumulation is a key condition for slope failure, independent of direct rainfall.
6. **Vegetation (NDVI)**: Vegetation cover, measured by the Normalized Difference Vegetation Index (NDVI), plays a protective role. Plant roots act as a natural binder for soil, enhancing its stability and preventing erosion. Areas with less vegetation are more exposed.
   - **Data Source**: MODIS/ MOD13Q1 Vegetation Index.
   - **Justification**: A weight of **0.10** acknowledges the protective but less direct role of vegetation compared to triggers like rainfall.
7. **Proximity to Drainage**: Areas near rivers and streams are susceptible to bank erosion and water-induced saturation, which can undercut slopes and cause instability.
   - **Data Source**: MERIT Hydro. This dataset provides high-resolution global hydrography data.
   - **Justification**: A weight of **0.05** was assigned, as this is a localized factor, but still contributes to risk.
8. **Aspect**: The direction of a slope influences its exposure to sun, wind, and rainfall. This can affect soil moisture and the type of vegetation present. For example, sun-facing slopes may be drier, while slopes exposed to prevailing winds and rain can be more saturated.
   - **Data Source**: Derived from the USGS SRTM DEM.
   - **Justification**: A small weight of **0.05** was given as its influence is more indirect and location-specific compared to other factors.
9. **Curvature**: The shape of the slope, whether it's convex (outward-curving) or concave (inward-curving), affects water flow and accumulation. Concave areas tend to concentrate water, increasing infiltration and risk.
   - **Data Source**: Derived from the USGS SRTM DEM.
   - **Justification**: A weight of **0.05** reflects its subtle but important role in local hydrology.

Classification into Zones: The final vulnerability image, with pixel values ranging from 0 to 1, is then reclassified into five distinct zones:

- **Low**: Score < 0.2
- **Moderate**: 0.4 ≤ Score < 0.6
- **High**: 0.6 ≤ Score < 0.8
- **Very High**: Score ≥ 0.8

7. The Foundational Role of Forests

Beyond their ability to make slopes more resistant to movement and erosion, forests play a crucial hydrological role. They function as natural sponges, absorbing and transpiring water from the soil, which significantly reduces the overall water content on a slope. In contrast, excessively saturated soil becomes heavy and unstable, dramatically increasing the likelihood of a landslide. By mitigating water infiltration, forests serve as a vital buffer against the very force that makes soil unstable.

Forest degradation, which includes outright deforestation for activities such as agriculture and urban development, directly undermines these protective functions. When a forest is cleared, the soil loses its natural anchor, leaving the ground loose, exposed, and highly vulnerable to being dislodged, particularly during intense monsoons. This connection between forest loss and landslides is especially pronounced in high-rainfall areas like the Himalayas, where the removal of tree cover allows rain to directly hit the ground, accelerating surface erosion and increasing the volume of water infiltrating the soil. This rapid rise in soil saturation can quickly lead to a slope's catastrophic failure.

The relationship between landslides and forest degradation can create a destructive feedback loop. While human-induced degradation can trigger a landslide, a major landslide event can, in turn, destroy vast tracts of forest. The immense force of the slide removes topsoil and vegetation, further reducing the landscape's ability to recover and making it even more susceptible to future disasters.

7.1 The Case of Himachal Pradesh

The data on forest cover in Himachal Pradesh serves as a tangible example of this challenge. As of the year 2000, the state's forested area was approximately 15,485 km². Over the subsequent two decades (2001–2020), Himachal Pradesh experienced a net forest loss of 75.3

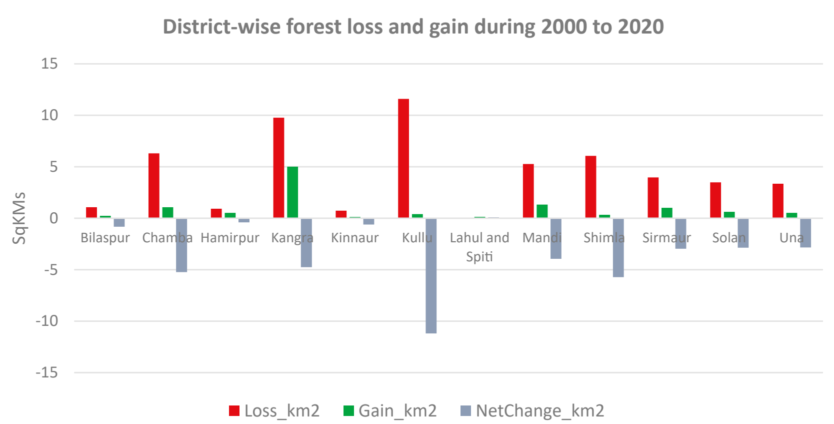

Graph-1: District-wise forest loss and gain during 2000 to 2020

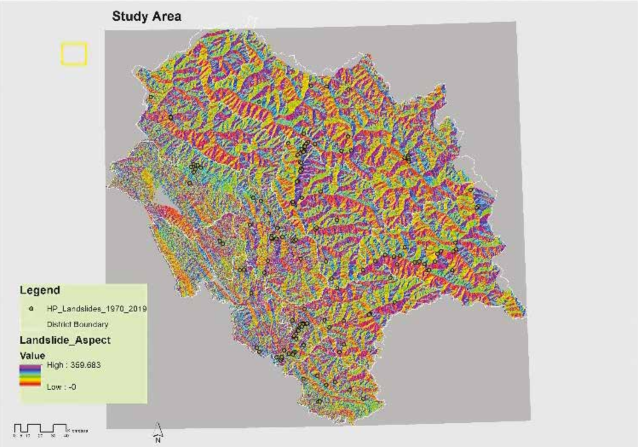

Map-2: Aspect of the study area

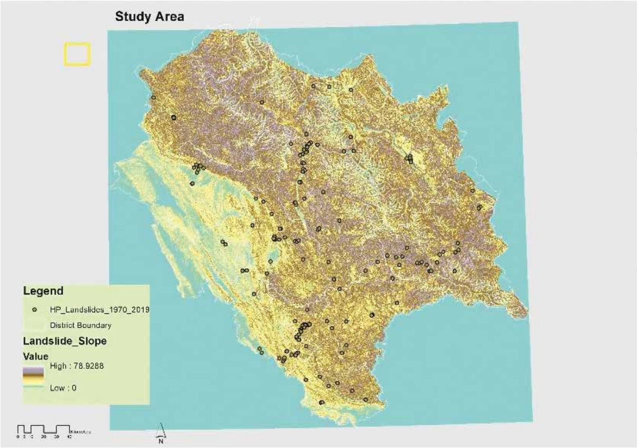

Map-3: Slope of the study area

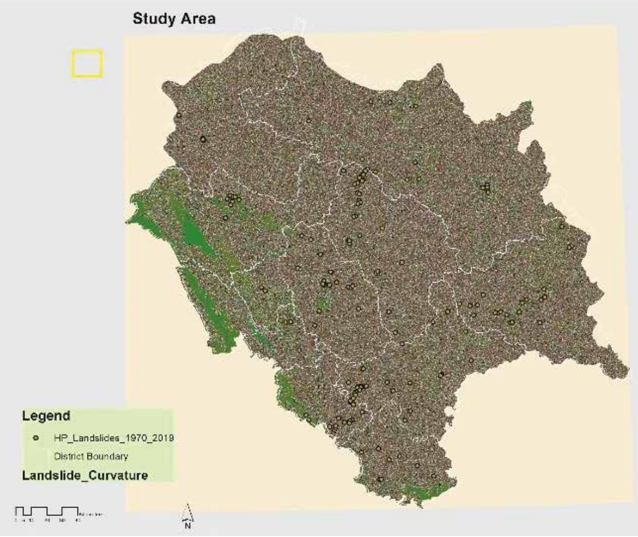

Map-4: Curveture of the study area

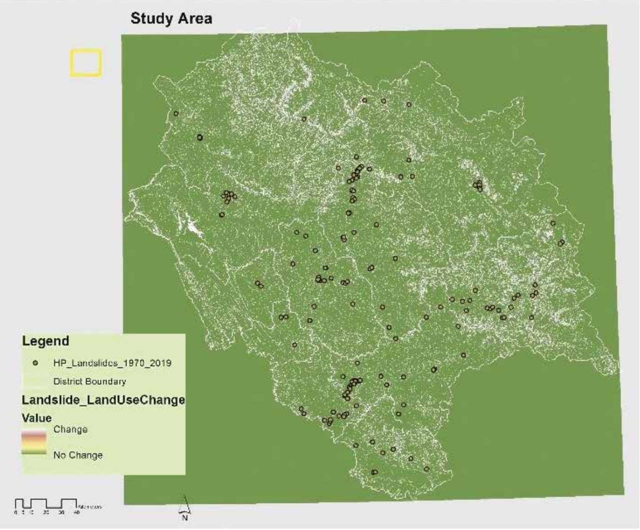

Map-5: Land Use Change (forest loss) of the study area

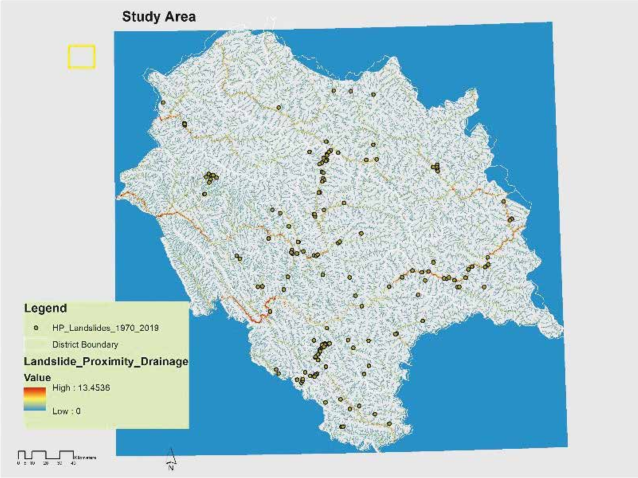

Map-6: Proximity to Drainge of the study area

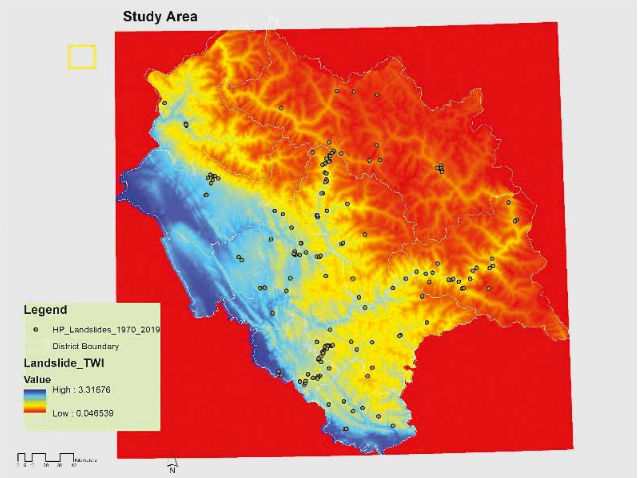

Map-7: TWI of the study area

km². While some areas saw gains through reforestation or natural regeneration, the loss of 91.4 km² outweighed these gains, resulting in a measurable reduction in forest cover. This decline represents a critical weakening of the region's natural defenses against landslides, placing both the natural environment and human communities in greater peril.

The data for forest changes in Himachal Pradesh comes from Global Forest Watch (GFW). GFW is a platform that tracks global forest change using satellite data. The core of their analysis is the Hansen et al. Global Forest Change dataset, which was created by a collaboration between the University of Maryland and Google using imagery from the Landsat satellite program.

8. Results and Limitations

The final vulnerability map provides a continuous index ranging from 0 (very low vulnerability) to 1 (very high vulnerability). The results highlight that the most vulnerable zones are concentrated in the mid-hills, where a combination of steep terrain, high rainfall, and dense human settlements overlap.

- **Kullu District** → High & Very High vulnerability in Beas Valley slopes, along NH-3 (Aut–Manali stretch), Banjar and Ani sub-divisions.
- **Mandi District** → High risk along Pandoh–Jogindernagar highway, Balh valley slopes.
- **Shimla District** → Vulnerability around Rampur–Narkanda road corridor, Shimla–Chopal belt.
- **Chamba District** → High risk in Bharmour and Churah regions.
- **Kinnaur District** → Very High risk in Sangla valley, Reckong Peo–Powari zone.

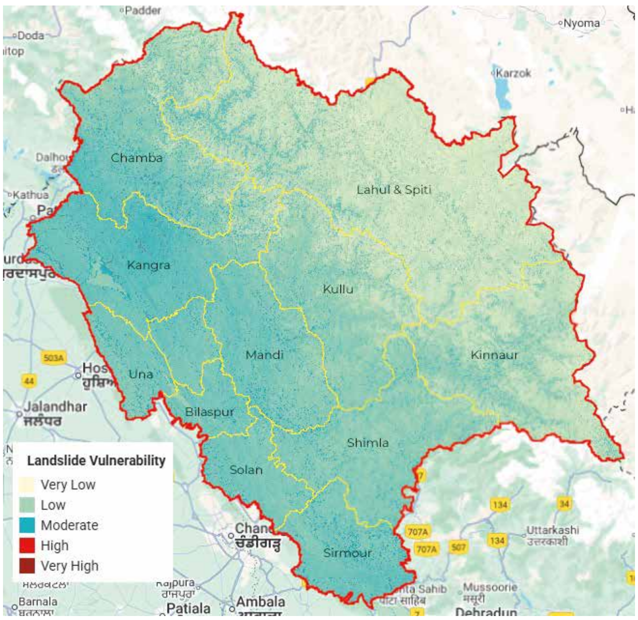

Map -8: Final Landslide Vulnerability Map

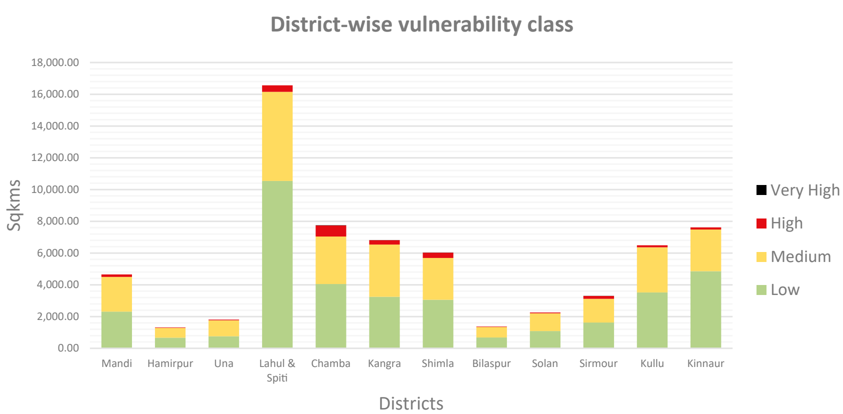

Graph-2: District-wise forest loss and gain during 2000 to 2020

9. Limitations:

- **Model Assumptions**: The weighted overlay model assumes that the selected weights are static and universally applicable across the entire study area, which may not hold true for all micro-climates and geological settings.
- **Data Resolution**: The 500-meter resolution of some datasets may not capture small-scale vulnerabilities.
- **Exclusion of Factors**: The current model doesn't incorporate crucial geological factors like lithology, fault lines, or seismic data, which are fundamental to understanding slope failure in the Himalayas.

10. Scope for Further Improvement

Future iterations of this project could significantly enhance accuracy and utility. Incorporating geological maps, historical landslide inventories, and seismic hazard data would provide a more complete picture of susceptibility. Using advanced machine learning models (e.g., Random Forest, Gradient Boosted Trees) could allow for a more data-driven determination of parameter weights, potentially identifying non-linear relationships between factors. Additionally, creating a near-real-time monitoring system that integrates recent satellite imagery and rainfall data could provide short-term landslide warnings.

11. Bibliography/References

- USGS. SRTM Digital Elevation Model.
- Climate Hazards Group. CHIRPS Daily Precipitation.
- European Space Agency. WorldCover.
- NASA. MODIS/MOD13Q1 Vegetation Index.
- Yamazaki, D. et al. (2019). MERIT Hydro: A high-resolution global hydrography map. Water Resources Research.

GNSS Constellation Specific Monthly Analysis Summary: September 2025

The analysis performed in this report is solely his work and own opinion. State Program: U.S.A (G); EU (E); China (C) "Only MEO- SECM satellites"; Russia (R); Japan (J); India (I)

Narayan Dhital
Actively involved to support international collaboration in GNSS-related activities. He has regularly supported and contributed to different workshops of the International Committee on GNSS (ICG), and the United Nations Office for Outer Space Affairs (UNOOSA). As a professional employee, the author is working as GNSS expert at the Galileo Control Center, DLR GfR mbH, Germany.

Introduction

This article continues the monthly performance analysis of the GNSS constellation. Readers are encouraged to refer to previous issues for foundational discussions and earlier results. In addition, there is a short overview on the recent anomaly and degradation in the UTC time dissemination parameter from GNSS broadcast messages.

Analyzed Parameters for September 2025

(**Dhital et. al, 2024**) provides a brief overview of the necessity and applicability of monitoring the satellite clock and orbit parameters.

a. Satellite Broadcast Accuracy, measured in terms of **Signal-In-Space Range Error (SISRE)** (**Montenbruck et. al, 2010**).
b. **SISRE-Orbit** (only orbit impact on the range error), SISRE (both orbit and clock impact), and **SISRE-PPP** (as seen by the users of carrier phase signals, where the ambiguities absorb the unmodelled biases related to satellite clock and orbit estimations. Satellite specific clock bias is removed) (**Hauschlid et.al, 2020**)
c. **Clock Discontinuity**: The jump in the satellite clock offset between two consecutive batches of data uploads from the ground mission segment. It is indicative of the quality of the satellite atomic clock and associated clock model.
d. **URA**: User Range Accuracy as an indicator of the confidence on the accuracy of satellite ephemeris. It is mostly used in the integrity computation of RAIM.
e. **GNSS-UTC offset**: It shows stability of the timekeeping of each constellation w.r.t the UTC
f. **UTC Offset Anomaly and Degradation:** It shows the anomaly in the difference between GNSS Time and Coordinated Universal Time (UTC) and is critical for converting GNSS Time to UTC in timing applications.

(a), (b) Satellite Clock and Orbit Accuracy (monthly RMS values)

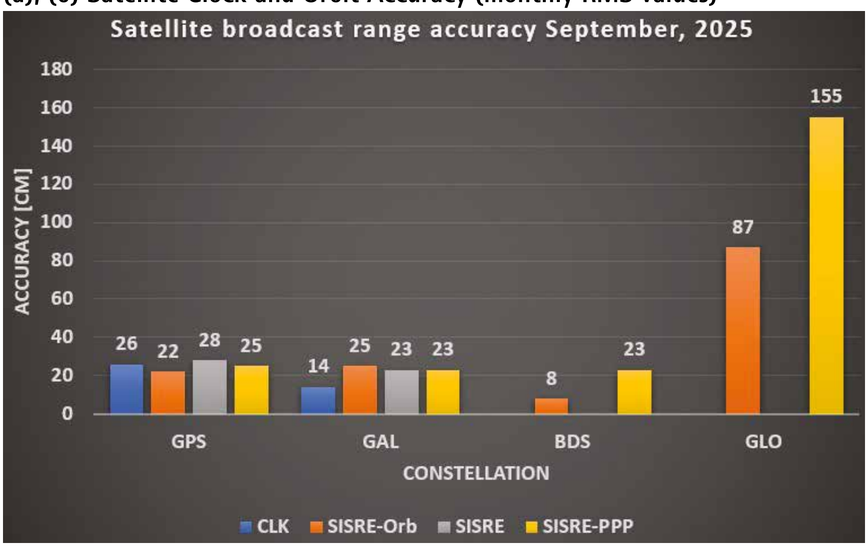

Note:- for India's IRNSS there are no precise satellite clocks and orbits as they broadcast only 1 frequency which does not allow the dual frequency combination required in precise clock and orbit estimation; as such, only URA and Clock Discontinuity is analyzed.

(c) Satellite Clock Jump per Mission Segment Upload

Const	Mean [ns]	Max [ns]	95_ Percentile [ns]	99_ Percentile [ns]	Remark (Best and Worst 95 %)
IRNSS	8.89	4924.47	5.60	57.93	Best I02 (4 ns) Worst I10 (17.39 ns) Big jumps for each satellite in multiple days.
GPS	12.36	156288.28	0.69	1.96	Best G16 (0.45 ns) Worst G03 (3.33 ns). The maximum jump was seen for G20 but that was covered by NANU. SVN51 started to transmit using PRN 20 from 30th September. The jump was related to that transition.
GAL	18.97	-	0.17	0.43	Best E03 (0.13 ns) Worst E19 (0.35 ns). Large discontinuity detected for E8 and E9 on one instance each. Further confirmation will be provided in next month's analysis.

(d) User Range Accuracy (Number of Occurrences in Broadcast Data 01-30 September)

IRNSS-SAT	2 [m]	2.8 [m]	4.0 [m]	5.7 [m]	8 [m]	8192 [m]	9999.9	Remark Other URA values (frequency)
I02	2909	6	1	-	1	1	-	-
I06	2880	23	9	-	2	-	-	-
I09	426	-	1	-	-	-	-	-
I10	1016	6	5	-	1	-	-	-

(e) GNSS-UTC Offset

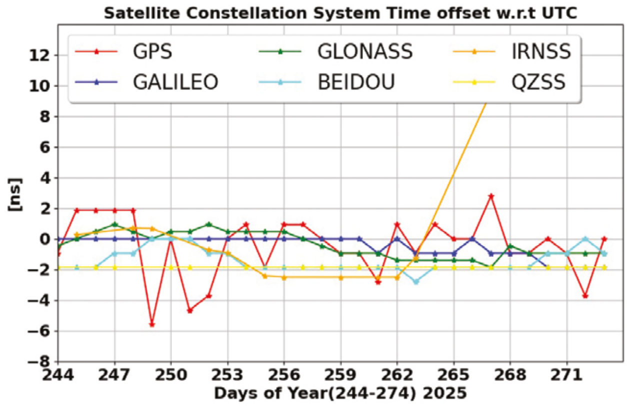

(F) Time Transfer Degradation: UTC Offset Anomaly and Degradation

The objective of this section is to highlight the necessity to monitor the GNSS-UTC broadcast parameter, as we have been doing every month in this column. Two examples from recent time are used to demonstrate the uses cases of the monitoring. On January 26, 2016, a GPS UTC anomaly occurred when 15 satellites began broadcasting incorrect UTC offset parameters—specifically the A0 and A1 coefficients (A1 impacted due to reference UTC week number set to 0) used to convert GPS Time to UTC (see **Equations 1-2** below). This led to a sudden ~13 microsecond discrepancy between GPS-derived UTC and actual UTC (**see Table F1**). The root cause was traced to a software update in the GPS ground control segment that mishandled the decommissioning of satellite SVN23. Although SVN23 was no longer active, its outdated UTC correction parameters were inadvertently propagated to active satellites during the update. This caused receivers that relied on the broadcast UTC offset to apply a faulty correction, resulting in timing errors (**Yao et.al, 2016**) Galileo and QZSS satellites were unaffected at the time, as they use independent timekeeping systems and did not broadcast erroneous UTC corrections during this period.

GNSS-UTC	A0	A1	DoY, 2016
GPUT	-4.6566128730e-09	-1.065814100e-14	023
GPUT	-6.5192580220e-09	-1.154631950e-14	024
GPUT	-9.3132257460e-10	5.329070520e-15	025
GPUT	-1.3696029780e-05	1.243449790e-14	026
GPUT	0.0000000000e+00	1.243449790e-14	027
GPUT	-9.3132257460e-10	3.552713680e-15	028
GPUT	-9.3132257460e-10	3.552713680e-15	029
GAUT	-4.6566128730e-09	8.881784200e-16	023
GAUT	-4.6566128730e-09	8.881784200e-16	024
GAUT	-3.7252902980e-09	8.881784200e-16	025
GAUT	-3.7252902980e-09	1.776356840e-15	026
GAUT	-3.7252902980e-09	1.776356840e-15	027
GAUT	-3.7252902980e-09	1.776356840e-15	028
GAUT	-3.7252902980e-09	8.881784200e-16	029
QZUT	1.8626451490e-08	-4.440892100e-15	023
QZUT	1.6763806340e-08	-6.217248940e-15	024
QZUT	1.6763806340e-08	-6.217248940e-15	025
QZUT	1.6763806340e-08	-4.440892100e-15	026
QZUT	1.7695128920e-08	-2.664535260e-15	027
QZUT	1.9557774070e-08	1.776356840e-15	028
QZUT	2.2351741790e-08	5.329070520e-15	029

Table F1: The UTC time dissemination error and frequency offset broadcast by each GNSS (GPS, Galileo and QZSS) from 23rd to 29th January 2016. On the 26th of January, the A0 (error in UTC time offset) had a large jump in microsecond level for GPS constellation (highlighted in red).

UTC=GPS Time- ΔUTC(t) (**Equation 1**)

ΔUTC(t)=A0+A1·(t-t_ref+ 604800(WN - WNt)) (**Equation 2**)

While this anomaly was mostly detected by the time laboratories, users of GPS timing receivers and GPS disciplined oscillators, it also pushed the GPS control segment for more robust approach in its UTC dissemination. For the positioning and navigation, however, the impact was not seen as the observables and residuals from the GPS signals can be used without the UTC information. Only the receivers that used the UTC offset to GPS from the navigation messages to convert from GPS to UTC time were impacted by the anomaly.

In the second example of the degradation of the GNSS-UTC dissemination, the events in **August–December 2023**, for Galileo constellation can be considered. The Galileo System Time (GST) drifted from UTC by up to **20 nanoseconds (see Figure F1)**, but still within the 30 ns requirement set by **Galileo Open Service standard** (**GSC et.al, 2023**). The degradation probably drifted the time synchronization process based only on GST. However, the prevalence of the multi-GNSS system meant it was not a big concern for the timing applications. To conclude, when these broadcast parameters (**Equation 2**) are incorrect/degraded, the computed UTC will deviate from true UTC. Not all receivers are impacted: positioning receivers use GNSS system time directly and are unaffected in terms of location accuracy. Timing receivers, however, become vulnerable if they apply the broadcast UTC offset without validation. NIST's UTC(NIST) was notably impacted in 2016 because several of its GPS-disciplined receivers trusted the faulty broadcast data. Other UTC(k) labs, especially those using multi-GNSS receivers or internal sanity checks, either avoided the error or recovered quickly. The Galileo 2023 anomaly similarly exposed the importance of cross-constellation validation and robust receiver design in safeguarding UTC(k) integrity.

The anomaly and degradation highlighted with these two examples reflect that even modern GNSS constellations can suffer timing inconsistencies. The physical realization of the time in the dedicated laboratories can also have issues that propagate to the values broadcast through the satellite. In our monthly monitoring of GNSS-UTC broadcast, such big anomaly or degradation have not been noticed so far, which is on a positive note, but some drifts in values for IRNSS and GLONASS have been noticed from time to time.

Monthly Performance Remarks:

1. Satellite Clock and Orbit Accuracy:
- The performance of GPS, Galileo and Beidou remained similar. The clock of Galileo improved by a small margin. GPS PRN 20 is resumed from 30th September and had a large clock jump on the day when SVN 51 started in transition to PRN20. NANU was released for the operational change. QZSS analysis is excluded for further consistency check in processing and to identify degradation in orbits of one of the QZSS satellites.
- IRNSS URA values for all satellites indicate improved accuracy.
- IRNSS clocks show I02 satellite has consistently good clock and I10 satellite has consistently the worst clock (note: among IRNSS satellite clocks)

2. The UTC Prediction (GNSS-UTC):
- All constellation, except IRNSS, provided relatively stable predictions of the GNSS-UTC. IRNSS started to drift heavily in the second half of the month.

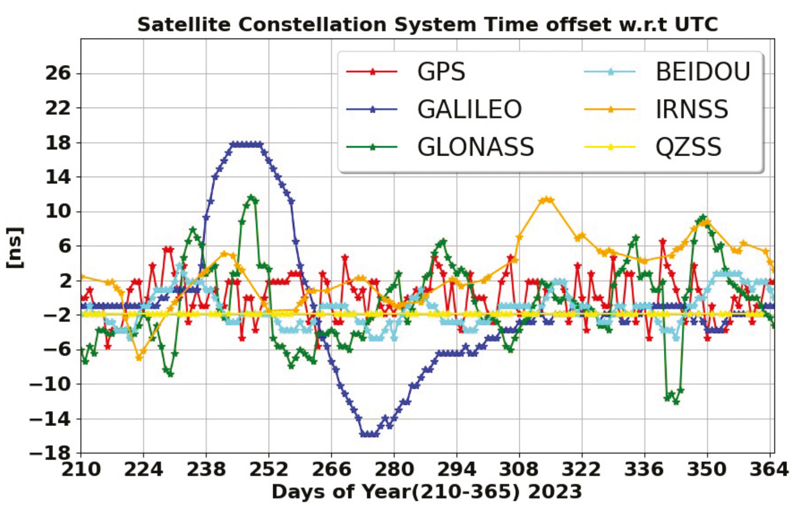

Figure F 1: The evolution of the UTC time dissemination offset as broadcast by different GNSS constellations. Galileo constellation had an unstable period during the second half of 2023. The offset computed by the UTC(k) of the Galileo system had a large deviation (up to 18 ns as indicated in the daily navigation message broadcast value).

References

Alonso M, Sanz J, Juan J, Garcia, A, Casado G (2020) Galileo Broadcast Ephemeris and Clock Errors Analysis: 1 January 2017 to 31 July 2020, MDPI

Alonso M (2022) Galileo Broadcast Ephemeris and Clock Errors, and Observed Fault Probabilities for ARAIM, Ph.D Thesis, UPC

Bento, M (2013) Development and Validation of an IMU/GPS/Galileo Integration Navigation System for UAV, PhD Thesis, UniBW.

BIMP (2024 a) https://e-learning.bipm.org/pluginfile.php/6722/mod_label/intro/User_manual_cggtts_analyser.pdf?time=1709905608656

BIMP (2024 b) https://e-learning.bipm.org/mod/folder/view.php?id=1156&forceview=1

BIMP (2024 c) https://cggtts-analyser.streamlit.app

Bruggemann, Troy & Greer, Duncan & Walker, R.. (2011). GPS fault detection with IMU and aircraft dynamics. IEEE Transactions on Aerospace and Electronic Systems - IEEE TRANS AEROSP ELECTRON SY. 47. 305-316. 10.1109/TAES.2011.5705677.

Cao X, Zhang S, Kuang K, Liu T (2018) The impact of eclipsing GNSS satellites on the precise point positioning, Remote Sensing 10(1):94

Chen, K., Chang, G. & Chen, C (2021) GINav: a MATLAB-based software for the data processing and analysis of a GNSS/IMU integrated navigation system. *GPS Solut* **25**, 108. https://doi.org/10.1007/s10291-021-01144-9

Curran, James T. & Broumendan, Ali. (2017). On the use of Low-Cost IMUs for GNSS Spoofing Detection in Vehicular Applications.

Dhital N (2024) GNSS constellation specific monthly analysis summary, Coordinates, Vol XX, Issue 1, 2, 3, 4

Dhital N (2025) GNSS constellation specific monthly analysis summary, Coordinates, Vol XXI, Issue 1

GINAv (2025). https://geodesy.noaa.gov/gps-toolbox/GINav.shtml

Goercke, L (2017) GNSS-denied navigation of fixed-wing aircraft using low-cost sensors and aerodynamic motion models, PhD Thesis, TUM.

GROOPS (2025) GROOPS Documentation and Cookbook. https://groops-devs.github.io/groops/html/index.html

GSC (2023) Galileo Q3 Performance Report. https://www.gsc-europa.eu/sites/default/files/sites/all/files/Galileo-OS-Quarterly-Performance_Report-Q3-2023.pdf

Guo, Jing & Chen, Guo & Zhao, Qile & Liu, Jingnan & Liu, Xianglin. (2017). Comparison of solar radiation pressure models for BDS IGSO and MEO satellites with emphasis on improving orbit quality. GPS Solutions. 21. 10.1007/s10291-016-0540-2.

Guo F, Zhang X, Wang J (2015) Timing group delay and differential code bias corrections for BeiDou positioning, J Geod,

Hauschlid A, Montenbruck O (2020) Precise real-time navigation of LEO satellites using GNSS broadcast ephemerides, ION

IERS C04 (2024) https://hpiers.obspm.fr/iers/eop/eopc04/eopc04.1962-now

IGS (2019) GNSS Attitude Quaternions Exchange using ORBEX

IGS (2021) RINEX Version 4.00 https://files.igs.org/pub/data/format/rinex_4.00.pdf

InsideGNSS (2024) Working papers: upgrading galileohttps://insidegnss.com/working-papers-upgrading-galileo/

Jiabo G, Xingyu Z, Yan C, Mingyuan Z (2021) Precision Analysis on Reduced-Dynamic Orbit Determination of GRACE-FO Satellite with Ambiguity Resolution, Journal of Geodesy and Geodynamics (http://www.jgg09.com/EN/Y2021/V41/I11/1127)

Kj, Nirmal & Sreejith, A. & Mathew, Joice & Sarpotdar, Mayuresh & Suresh, Ambily & Prakash, Ajin & Safonova, Margarita & Murthy, Jayant. (2016). Noise modeling and analysis of an IMU-based attitude sensor: improvement of performance by filtering and sensor fusion. 99126W. 10.1117/12.2234255.

Li M, Wang Y, Li W (2023) performance evaluation of real-time orbit determination for LUTAN-01B satellite using broadcast earth orientation parameters and multi-GNSS combination, GPS Solutions, Vol 28, article number 52

Li W, Chen G (2023) Evaluation of GPS and BDS-3 broadcast earth rotation parameters: a contribution to the ephemeris rotation error Montenbruck

Liu, Yue & Liu, Fei & Gao, Yang & Zhao, Lin. (2018). Implementation and Analysis of Tightly Coupled Global Navigation Satellite System Precise Point Positioning/Inertial Navigation System (GNSS PPP/IMU) with IMUfficient Satellites for Land Vehicle Navigation. Sensors. 18. 4305. 10.3390/s18124305.

Mayer-Guerr, T., Behzadpour, S., Eicker, A., Ellmer, M., Koch, B., Krauss, S., Pock, C., Rieser, D., Strasser, S., Suesser-Rechberger, B., Zehentner, N., Kvas, A. (2021). GROOPS: A software toolkit for gravity field recovery and GNSS processing. Computers & Geosciences, 104864. https://doi.org/10.1016/j.cageo.2021.104864

Montenbruck O, Steigenberger P, Hauschlid A (2014) Broadcast versus precise ephemerides: a multi-GNSS perspective, GPS Solutions

Liu T, Chen H, Jiang Weiping (2022) Assessing the exchanging satellite attitude quaternions from CNES/CLS and their application in the deep eclipse season, GPS Solutions 26(1)

Montenbruck O, Steigenberger P (2024) The 2024 GPS accuracy improvement initiatives, GPS Solutions

Montenbruck O, Steigenberger P, Hauschlid A (2014) Broadcast versus precise ephemerides: a multi-GNSS perspective, GPS Solutions

Montenbruck O, Hauschlid A (2014 a) Differential Code Bias Estimation using Multi-GNSS Observations and Global Ionosphere Maps, ION

Montenbruck, O., Schmid, R., Mercier, F., Steigenberger, P., Noll, C., Fatkulin, R., Kogure, S. & Ganeshan, A.S. (2015) GNSS satellite geometry and attitude models. Advances in Space Research 56(6), 1015-1029. DOI: 10.1016/j.asr.2015.06.019

Niu, Z.; Li, G.; Guo, F.; Shuai, Q.; Zhu, B (2022) An Algorithm to

Assist the Robust Filter for Tightly Coupled RTK/IMU Navigation System. *Remote Sens*. **2022**, *14*, 2449. https://doi.org/10.3390/rs14102449

Schmidt, G, Phillips, R (2010) IMU/GPS Integration Architecture Performance Comparisons. NATO.

Space (2025) https://www.space.com/astronomy/earth/mysterious-boost-to-earths-spin-will-make-aug-5-one-of-the-shortest-days-on-record

Steigenberger P, Montenbruck O, Bradke M, Ramatschi M (2022) Evaluation of earth rotation parameters from modernized GNSS navigation messages, GPS Solutions 26(2)

Strasser S (2022) Reprocessing Multiple GNSS Constellations and a Global Station Network from 1994 to 2020 with the Raw Observation Approach, PhD Thesis, Graz University of Technology

Suvorkin, V., Garcia-Fernandez, M., González-Casado, G., Li, M., & Rovira-Garcia, A. (2024). Assessment of Noise of MEMS IMU Sensors of Different Grades for GNSS/IMU Navigation. *Sensors*, *24*(6), 1953. https://doi.org/10.3390/s24061953

Sylvain L, Banville S, Geng J, Strasser S (2021) Exchanging satellite attitude quaternions for improved GNSS data processing consistency, Vol 68, Issue 6, pages 2441-2452

Tanil, Cagatay & Khanafseh, Samer & Pervan, Boris. (2016). An IMU Monitor agaIMUt GNSS Spoofing Attacks during GBAS and SBAS-assisted Aircraft Landing Approaches. 10.33012/2016.14779.

Walter T, Blanch J, Gunning K (2019) Standards for ARAIM ISM Data Analysis, ION

Wang, C & Jan, S (2025). Performance Analysis of MADOCA-Enhanced Tightly Coupled PPP/IMU. NAVIGATION: Journal of the IMUtitute of Navigation March 2025, 72 (1) navi.678; DOI: https://doi.org/10.33012/navi.678

Wang N, Li Z, Montenbruck O, Tang C (2019) Quality assessment of GPS, Galileo and BeiDou-2/3 satellite broadcast group delays, Advances in Space Research

Wang J, Huang S, Lia C (2014) Time and Frequency Transfer System Using GNSS Receiver, Asia-Pacific Radio Science, Vol 49, Issue 12

https://cggtts-analyser.streamlit.app

Yang N, Xu A, Xu Z, Xu Y, Tang L, Li J, Zhu H (2025) Effect of WHU/GFZ/CODE satellite attitude quaternion products on the GNSS kinematic PPP during the eclipse season, Advances in Space Research, Volume 75, Issue 1,

Yao J, Lombardi M, Novick A, Patla B, Sherman J, Zhang V (2016) The effects of the January 2016 UTC offset anomaly on GPS-controlled clocks monitored at NIST. https://tf.nist.gov/general/pdf/2886.pdf

Note: References in this list might also include references provided to previous issues.

Data sources and Tools:

https://cddis.nasa.gov (Daily BRDC); http://ftp.aiub.unibe.ch/CODE_MGEX/CODE/ (Precise Products); BKG “SSRC00BKG” stream; IERS C04 ERP files

(The monitoring is based on following signals- GPS: LNAV, GAL: FNAV, BDS: CNAV-1, QZSS:LNAV IRNSS:LNAV GLO:LNAV (FDMA))

Time Transfer Through GNSS Pseudorange Measurements: https://e-learning.bipm.org/login/index.php

Allan Tools, https://pypi.org/project/AllanTools/gLAB GNSS, https://gage.upc.edu/en/learning-materials/software-tools/glab-tool-suite

JAXA choses ArkEdge Space to study LEO PNT system

ArkEdge Space Inc., a Japanese space startup based in has been selected by the Japan Aerospace Exploration Agency (JAXA) to conduct the “Study of Key Technologies and Related Systems for the Dedicated Low Earth Orbit Positioning, Navigation, and Timing (LEO-PNT) system.” The LEO-PNT system will comprise a constellation of small satellites in low Earth orbit (500–1,200 km), significantly closer to Earth than conventional GNSS which orbit at approximately 20,000 km. Operating at lower altitudes is expected to enable the delivery of high-intensity and higher-accuracy positioning information services globally.

LEO-PNT’s high-intensity positioning signals are expected to complement the weak signal strength of conventional GNSS signals reaching the Earth’s surface, which are more susceptible to interference. With threats such as jamming and spoofing becoming increasingly prominent, the more accurate and reliable positioning information provided by LEO-PNT is also expected to be used in many other fields.

This study builds on JAXA’s Feasibility Study on LEO-PNT (Part 1) conducted from October 2024 to March 2025. The new effort will further advance research into key technologies and system concepts required to establish a robust, GNSS-independent alternative PNT capability.

The study will particularly focus on designing resilient PNT architectures capable of maintaining operations even when GNSS is disrupted. It will also address the design and transmission of robust LEO-PNT signals, including both ranging signals and navigation messages, across multiple frequency bands such as the C-band (C1: 5010–5030 MHz, C2–4: 5030–5250 MHz), S-band, and L-band. *arkedgespace.com*

Exploring the maritime archaeology of Guadalcanal and Iron Bottom Sound

The Ocean Exploration Trust (OET)'s exploration vessel (E/V) Nautilus is underway on its third expedition of 2025 to conduct archaeological surveys of historically significant shipwrecks in the Iron Bottom Sound - the site of five famous naval battles, which were a turning point in the WWII Pacific theater. Led by OET President and famed explorer Dr. Robert Ballard, the 21-day expedition will utilize OET's remotely operated vehicles (ROVs) in combination with the mapping capabilities of the University of New Hampshire's uncrewed surface vessel (USV) DriX. This coordinated technology approach aboard E/V Nautilus demonstrates new efficiencies in archaeological ocean exploration supported by NOAA Ocean Exploration via the Ocean Exploration Cooperative Institute.

"I am looking forward to returning to Iron Bottom Sound, which I first explored in 1991 and 1992 when we discovered 12 lost Australian, Japanese, and American warships," says Ballard. "This time we have a much more impressive array of undersea and surface vehicle systems and advanced acoustical and imaging systems needed to locate and document many of the warships and aircraft remaining to be discovered."

Located in the Solomon Islands, Iron Bottom Sound was the stage of five major naval battles between August and December 1942, which resulted in the loss of over 20,000 lives, 111 naval vessels, and 1,450 planes from the Allied forces and the Empire of Japan. These underwater maritime heritage sites now rest on the seafloor in a confined area offshore Honiara, less than 25 nautical miles wide and 40 nautical miles long. To date, only 30 of the military ships lost in this area have been located, with at least 21 remaining to be found within the deep waters of Iron Bottom Sound.

"NOAA Ocean Exploration's mission is to explore the ocean for America's benefit," said Captain William Mowitt of the NOAA Corps, acting director of NOAA Ocean Exploration. "By pairing cutting-edge technologies like DriX with OET's deep-diving ROVs, we have the potential to reshape our understanding of what lies in the deep ocean, from undiscovered shipwrecks to untapped resources."

Exploration of Iron Bottom Sound has been underway for more than 30 years. Past missions aimed to find and identify wrecks, but further exploration is needed, focusing on sites that have not yet been imaged at a higher resolution.

On this expedition, USV DriX will gather data for a more detailed map than ever before of the entire Iron Bottom Sound to identify exploration sites.

The team will then utilize the advanced camera systems of ROVs Hercules and Atalanta to conduct non-invasive archaeological surveys, assessing the condition of each wreck, its significance as an artificial reef, as well as identifying potential sources of marine pollution.

"It will be both humbling and very sobering to map out the extent of destruction that lies at the bottom of Iron Bottom Sound while recognizing the thousands of lives that were lost there and the significance of the sacrifices made," says Dr. Larry Mayer, Director, Center for Coastal and Ocean Mapping at the University of New Hampshire.

Eighty years after the war, this expedition brings together archaeological experts from all former combatant nations — the United States, Japan, Australia, and New Zealand— as well as interdisciplinary experts worldwide through the Scientist Ashore program. In locating and exploring these historically significant sites, this expedition aims to honor those lost and keep alive the memory of sacrifices made during the Battles of Guadalcanal, as well as highlight the significance of this unique place globally.

"Iron Bottom Sound was the scene of five ferocious major night surface battles resulting in the loss of dozens of ships and thousands of men. Both sides fought with extreme courage and tenacity, although in the end the U.S. Navy and allies prevailed, at enormous cost," said Naval History and Heritage Command Director Samuel J.

Cox, U.S. Navy rear admiral (retired). "These wrecks represent the last resting place of sailors who gave the last full measure of devotion in the service of

E V Nautilus & DriX – Credit Ocean Exploration Trust

their country. This expedition is an opportunity to remember the valor and sacrifice of those who turned the tide of war in favor of freedom, especially those who never returned home."

The Maritime Archaeology of Guadalcanal expedition is supported by NOAA Ocean Exploration via the Ocean Exploration Cooperative Institute. This exploration is made possible by the expertise, support, and collaboration of many partners, including NOAA Ocean Exploration, U.S. Naval History and Heritage Command, Solomon Islands government, University of New Hampshire Center for Coastal and Ocean Mapping/Joint Hydrographic Center, and Japanese, Australian, and New Zealand colleagues.

The expedition will be streamed live on NautilusLive.org, a 24-hour platform that brings ocean exploration directly to viewers on shore. Telepresence technology allows viewers to engage with the team at sea, asking questions and receiving realtime behind-the-scenes updates via social media. Classrooms worldwide are invited to connect with the at-sea team via free educational Q&A interactions.

After this expedition, the OET 2025 field season will continue with exploration of the Republic of the Marshall Islands and Wake Atoll. OET's 2025 expeditions will build ocean knowledge supporting international scientific and U.S. governmental priorities, particularly understanding the deep sea, sharing that knowledge with others, and contributing new discoveries and data to inform future resource management decisions. Through the open sharing of data collected during these expeditions, OET directly contributes to the US National Strategy for Ocean Mapping, Exploration, and Characterization, the Beyond the Blue: Illuminating the Pacific campaign, and other coordinated initiatives.

About the Ocean Exploration Trust

The Ocean Exploration Trust was founded in 2007 by Dr. Robert Ballard to explore the ocean, seeking out multidisciplinary discoveries while pushing the boundaries of STEAM education and technological innovation. Our international program is launched from aboard the Exploration Vessel (E/V) Nautilus, offering live exploration to participants on shore and the public via live video, audio, and data feeds. Learn more about Ocean Exploration Trust.

The 2025 E/V Nautilus expeditions are primarily sponsored by NOAA Ocean Exploration via the Ocean Exploration Cooperative Institute. OET program sponsors and partners for 2025 also include the Office of Naval Research, QPS, and the Phillip Stephenson Foundation.

https://nautiluslive.org/blog/2025/06/30/exploring-maritime-archaeology-guadalcanal-and-iron-bottom-sound

Japan model inspires India's spatial policy for urban planning

The new National Spatial Policy envisions 20-year urban blueprints, regional planning blocks, and transit-led growth to curb haphazard expansion and boost liveability across Indian cities. The three tiers will have proper policy frameworks. Taking a leaf out of Japan's urban planning and governance playbook, India has framed a National Spatial Policy (NSP) to plan new cities, redevelop older cities, and align state and city planning with economic growth and liveability.

The ministry of housing and urban affairs has framed the policy, which will develop 20-year vision documents for city planning and create structures from regional to national level for implementation of the framework in a cohesive manner. The need for the NSP stems from projections of urban population living in cities – which is likely to grow from 30 per cent to about 52-53 per cent in 20 years. The NSP proposes a three-tier system – creation of a National Spatial Coordination Council (which will have representatives of line ministries, PMO and Niti Aayog), a State Spatial Strategy which will have a state-level group and a regional planning block which will be governed by a regional planning body.

According to sources, the NSP has proposed around 50 regional planning blocks, anchored in million-plus city regions. The NSP will set 20-year goals, a national structure, corridor maps, climate risk principles, and investment priorities. Every regional plan will include economic vision and growth drivers, infrastructure plan, natural resource and environment plan and climate action plan. Every city will also have a mandatory plan.

Two major thrust areas are land use and the transport system. The policy proposes that all states should employ a transit-first and rail-led growth at the core. This means making public transport like mass transit corridors, Metro, RRTS and railway the primary arteries of urbanisation while highways are regulated as freight and logistics corridors.

The policy also proposes employing the Japanese concept of 'Kukaku Seiri', a principle of reallocation of land. This is used for transformation of unplanned urbanised areas on the fringe of cities. In this, land is exchanged among the owners and is consolidated for each owner, whilst some of the land is reserved for public facilities.

So overall, a landowner may lose small portions of land but the net worth increases as the government develops facilities and the cost of land rises. "For the government it means a more planned city rather than growth of urban slums," said the official. The NSP also proposes redeveloping existing cities through comprehensive upgrades of legacy infrastructure (water, sewerage, housing, power and transport systems). *https://infra.economictimes.indiatimes.com*

Department of Posts signs MoU with ESRI India

The Department of Posts (DoP), has signed a Memorandum of Understanding (MoU) with ESRI India. Under this MoU, DoP will be able to use Esri India's high-resolution imagery and street basemaps for its DIGIPIN portal. The collaboration will also enable the integration of DIGIPIN with Esri India's Living Atlas portal, thereby making it accessible to the larger GIS community. Further, ESRI India will provide technical support to the DoP for seamless integration of their services for DIGIPIN. *www.pib.gov.in*

Verra releases innovative digital soil mapping tool

Verra has published a digital soil mapping (DSM) tool - VT0014 Estimating organic carbon stocks using digital soil mapping, version 1.0 provides guidance for the development, calibration, and validation of data-driven modeling methods to estimate soil organic carbon (SOC) stocks in a spatially explicit manner, including model uncertainty estimations. Because the tool is based on robust, up-to-date science and novel technologies, such as remote sensing, it enables ALM projects to generate high-integrity carbon credits. *verra.org*

NASA-ISRO satellite sends first radar images of earth's surface

The NISAR (NASA-ISRO Synthetic Aperture Radar) Earth-observing radar satellite's first images of our planet's surface are in, and they offer a glimpse of things to come as the joint mission between NASA and ISRO (Indian Space Research Organisation) approaches full science operations later this year. Images from the spacecraft, which was launched by ISRO on July 30, display the level of detail with which NISAR scans Earth to provide unique, actionable information to decision-makers in a diverse range of areas.

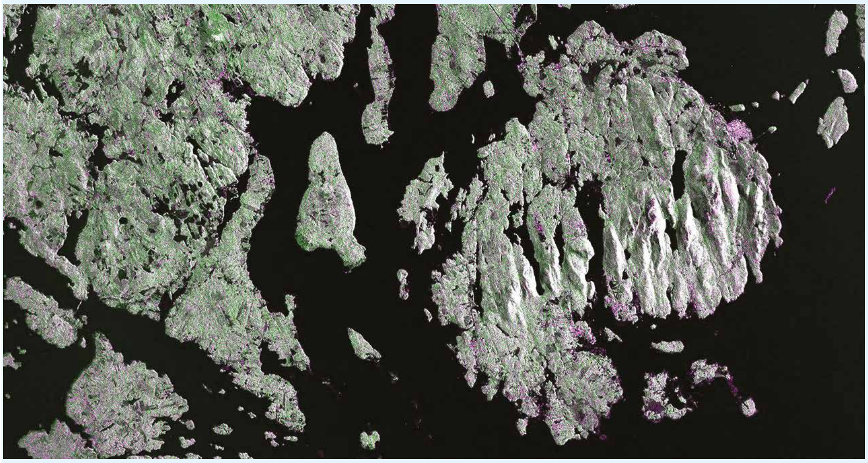

On Aug. 21, the satellite's L-band synthetic aperture radar (SAR) system, which was provided by NASA's Jet Propulsion Laboratory in Southern California, captured Mount Desert Island on the Maine coast. Dark areas represent water, while green areas are forest, and magenta areas are hard or regular surfaces, such as bare ground and buildings. The L-band radar system can resolve objects as small as 15 feet (5 meters), enabling the image to display narrow waterways cutting across the island, as well as the islets dotting the waters around it.

Then, on Aug. 23, the L-band SAR captured data of a portion of northeastern North Dakota straddling Grand Forks and Walsh counties. The image shows forests and wetlands on the banks of the Forest River passing through the center of the frame from west to east and farmland to the north and south. *www.nasa.gov/news-release/nasa-isro-satellite-sends-first-radar-images-of-earths-surface.*

Taiwan dispatches remote sensing satellites to US

Taiwan shipped the first satellite of its next-generation FORMOSAT-8 Earth-observation program to the US on Tuesday for a planned fourth-quarter launch, according to the Taiwan Space Agency (TASA).

Officials hailed the send-off as a milestone for Taiwan's space ambitions. The spacecraft has been dubbed the "Chi Po-lin Satellite," honoring the late aerial filmmaker whose documentary "Seeing Taiwan" raised public focus on the island's environment. The launch will begin deployment of an eight-satellite constellation designed to provide frequent imaging of Taiwan and the wider region. The remaining units are expected to roll out over several years, with full deployment targeted by 2031. *www.aa.com.tr*

UAE-France cooperation

The Emirati National Space Science and Technology Center (NSSTC) and U-Space, a French smallsat constellation manufacturer, signed a major contract for the design and manufacture of a turnkey 12U satellite. It will be the precursor of a future constellation dedicated to the Emirati LEONAV programme, which aims at deploying a Low Earth Orbit, Positioning, Navigation and Timing (LEO PNT) service. This contract is a major milestone for the NSSTC to demonstrate the delivery of a LEO PNT service in the area. *www.u-space.fr*

New Iranian satellite set for launch

Hossein Shahrabi, CEO of a knowledge-based company that has manufactured the satellite, told Tasnim that it has been designed as a follow-up to Kowsar and Hodhod satellites, incorporating the combined missions of both. He explained that Dual-View 1 is designed to function as Iran's first integrated remote sensing and communications satellite within a planned constellation.

The upgraded model features additional solar cells and improved communications hardware. From the three communications links used in Kowsar and Hodhod, the most effective have been integrated into the new satellite, along with the addition of an S-band link, enabling full ground-based attitude control programming, he added. Shahrabi said Dual-View 1 is scheduled for launch in the Iranian month of Azar (November 22 – December 21) with the same launcher previously used for Kowsar and Hodhod. *https://en.mehrnews.com*

UK rail network to be monitored from space

SatSense has secured a landmark multi-million-pound, multi-year contract with Network Rail to deliver network-wide ground deformation monitoring, flood mapping and change detection services using satellite radar technology. This is the first time globally that integration of satellite-based ground monitoring has been undertaken at this scale by a major rail operator. The innovative approach paves the way for redefining geotechnical asset management and setting a new standard for sustainable infrastructure monitoring.

Under the agreement, SatSense will deliver processed InSAR data and derived services that integrate into Network Rail's earthwork asset management systems, utilizing data from satellites such as the Sentinel-1, NISAR and TerraSAR-X constellations. The approach aims to enable a transition to reduce reliance on repeat on-site examinations which can be costly, subjective and untimely. *satsense.com*

Australian nanosatellite snaps 1st selfie

The first image taken by the SpIRIT selfie camera, acquired over New Zealand at the end of the thermal radiator deployment sequence. (Image credit: University of Melbourne (Australian University)

The first image taken by the SpIRIT selfie camera, acquired over New Zealand at the end of the thermal radiator deployment sequence. (Image credit: University of Melbourne (Australian University)

Australia's SpIRIT nanosatellite has snapped its first "selfie" from space, marking a successful start to its mission.

SpIRIT — formally known as the Space Industry Responsive Intelligent Thermal nanosatellite — is the first space telescope funded by the Australian Space Agency to carry a foreign space agency's scientific instrument as its main payload.

Launched in December 2023 aboard a SpaceX Falcon 9 rocket, SpIRIT has now completed its commissioning phase, testing all its onboard systems, including its winged thermal management and deployable camera arm, which it used to take a "selfie" in space.

Recent images shared by the University of Melbourne show the satellite in orbit, confirming that its systems were deployed and are functioning correctly. The images include snapshots of the satellite's thermal radiator, electric propulsion thruster payload, telecommunication transceivers and solar panels. *www.space.com*

Study on GNSS authentication and security improvements

The E-GIANTS (European GNSS Improved Authentication Solutions) project was commissioned by the European Commission and technically supervised by EUSPA. The project responds to the growing threat posed by quantum computing to traditional cryptographic methods, which could compromise the security of GNSS services in the coming decade. The study highlights that while quantum computers threaten classic asymmetric cryptography (like RSA and ECDSA), symmetric mechanisms—properly configured—remain secure, guiding the project's design choices.

The project's scope encompassed three main work objectives:

1. SBAS and OSNMA Key Management: Focused on developing a comprehensive authentication solution for Satellite-Based Augmentation Systems (SBAS) and the Galileo OSNMA (Open Service Navigation Message Authentication) service, using symmetric cryptography to ensure bandwidth efficiency and post-quantum resilience. The solution centres on a TESLA-based (Timed Efficient Stream Loss-tolerant Authentication) protocol, optimised for low authentication latency (about 1 second) and robust message recovery using Reed-Solomon encoding.

2. Additional Dissemination and Improvements of OSNMA: Proposed and validated improvements to the Galileo OSNMA protocol, including the distribution of cryptographic material via secure internet protocols (MQTTS and NTPs) for receivers with connectivity. These enhancements reduce authentication delays, improve cold-start performance, and introduce strategies for cross-constellation authentication, paving the way for integrating GPS and Galileo authentication in the future. The project also explored post-quantum resistant Merkle tree architectures for OSNMA, though further study is needed for large-scale deployment.

3. SBAS Authentication for Non-Aviation Users: Extended authentication solutions to new SBAS services (EGNOS-Next), particularly for non-aviation sectors like maritime, road, and rail. The approach adapts the TESLA-based protocol to high data rate channels (E5C/E5D), ensuring rapid, authenticated access to critical navigation and integrity messages for a broader user base.

Key outcomes of the project include:

- **Post-Quantum Resilience:** By relying on symmetric cryptography and hash-based structures, the solutions are designed to withstand attacks from future quantum computers, avoiding the bandwidth-heavy hybridisation of classic and post-quantum asymmetric algorithms.
- **User-Centric Design:** Extensive stakeholder interviews shaped requirements, emphasising minimal receiver hardware/software impact, low authentication delays, and standardised, interoperable solutions.
- **Enhanced OSNMA Protocol:** The project identified improvements to the OSNMA framework, including asynchronous broadcasting of subframes across the Galileo constellation. This ensures more consistent authentication performance, even in areas with limited satellite visibility. Additionally, the proposal for cross-constellation authentication aims to extend OSNMA's capabilities to non-Galileo satellites, enhancing its versatility.
- **Secure Data Distribution:** A new method for distributing cryptographic material to GNSS receivers with internet connectivity was introduced, identifying MQTTS (Message Queuing Telemetry Transport over TLS) and NTPs (Network Time Protocol) as the most suitable network protocols. The implementation of non-SIS services, either independently or in conjunction with SIS, was found to improve authentication, especially in challenging environments.
- **System-Level Roadmap:** A detailed deployment plan was developed, outlining a roadmap for standardisation, prototyping, and phased implementation, aligning with EGNOS V3 service upgrades and future GNSS receiver capabilities. The roadmap emphasises security analysis, system design, and integration with existing GNSS infrastructure.
- **Key Management Innovations:** The project addressed vulnerabilities in current cryptographic practices, including the risk of quantum computing threats to classical asymmetric algorithms like ECDSA. Recommendations for resilient key management strategies were proposed to future-proof authentication systems.

By integrating these advancements, the project underscores the importance of robust authentication in maintaining the integrity of GNSS services. The findings and technical proposals from E-GIANTS will contribute to the evolution of Galileo and EGNOS's capabilities, ensuring its role as a trusted enabler for critical infrastructure across Europe and beyond.

The E-GIANTS consortium recommends further prototyping and experimentation to validate full-scale implementations, as well as continued analysis of internet-based cryptographic material distribution and time synchronization services. Standardization activities are underway to harmonize these authentication mechanisms across European and global SBAS systems. *www.euspa.europa.eu*

Japan to launch another positioning satellite

The Japan Aerospace Exploration Agency (JAXA) and Mitsubishi Heavy Industries will launch an additional Michibiki positioning satellite aboard an H3 rocket on Dec. 7.

The launch is scheduled to take place between 11:30 a.m. and 12:30 p.m. from the Tanegashima Space Center in Kagoshima Prefecture. The Michibiki satellite system serves as the Japanese version of GPS, offering precise positioning to centimeter-level. Currently, five Michibiki satellites are in operation. *www.japantimes.co.jp*

Galileo R&D tests new uplink antenna

Galileo relies on ground-based uplink stations (ULS) to maintain accurate positioning for users worldwide. These stations transmit essential data to the satellites, including the information required to compute the satellites' orbits and clock corrections. Traditionally, such messages are sent using dish antennas. However, a new type of ground uplink antenna – a phased array antenna – was recently tested at the European Space Agency's (ESA) site in Redu, Belgium.

While traditional ground stations, using dish antennas, rely on mechanical steering to track and maintain contact with a single satellite, phased array antennas use electronics to steer the radio waves and communicate with satellites. This enables faster satellite pointing and re-pointing, improved reliability over the station's lifetime and simultaneous communication with multiple satellites.

The ability of one phased array antenna to contact multiple satellites at once could be useful for satellite constellations, such as Galileo Second Generation (G2), which is currently under development. Phased array antennas for uplink could be a more efficient system capable of transmitting more data to more satellites. This could support new and improved services and reduce the number of ground stations and amount of maintenance needed. *www.esa.int*

ESA inaugurates new deep space antenna in Australia

At an Oct. 4 event in New Norcia, Western Australia, ESA marked the completion of a new 35-meter antenna for communicating with spacecraft throughout the solar system. The antenna is the second at New Norcia and the fourth in ESA's Estrack network worldwide. It is called New Norcia 3 and will support communications with ESA spacecraft once it begins operations, expected next March. *spacenews.com*

ICAO Assembly condemns GNSS radio frequency interference

The ICAO Assembly has endorsed the determination of its governing Council that recurring incidents of GNSS Radio Frequency Interference (RFI) originating from the Democratic People's Republic of Korea (DPRK) and the territory of the Russian Federation constitute infractions of the 1944 Convention on International Civil Aviation.

Through two Resolutions, the ICAO Assembly condemned the DPRK and the Russian Federation for the infractions and urgently called upon them to comply strictly with their obligations under the Convention. The Assembly also deplored the fact that incidents of GNSS RFI originating from the DPRK and the Russian Federation have continued to recur in disregard of the concerns repeatedly expressed by the ICAO Council about the harmful impact of GNSS-RFI on the safety and security of international civil aviation.

The Assembly reiterated the paramount importance of preserving the safety and security of international civil aviation through strict compliance with the principles enshrined in the Chicago Convention and its Annexes. It also recalled Assembly Resolution A41-8, which recognized that the spectrum used by GNSS should be free from harmful interference and urged States to refrain from any form of jamming or spoofing affecting civil aviation. *www.icao.int*

NSI field-tests specialized navigation software

The Virginia Tech National Security Institute (VTNSI) is helping plot a course toward safe navigation when traditional GPS fails.

Researchers in the institute's Mission Systems Division recently kicked off a series of field-tests aimed at further validating the magnetic field-based geolocation software patented by AstraNav. The company's software-based magnetic-field based geolocation solution (M-GPS), aims to provide devices and vehicles with reliable, accurate navigational data, including in GPS-denied and network-denied environments. Testing of the software is being carried out across land, sea, and air systems, including underwater uncrewed vehicles, uncrewed aerial systems, and crewed aircraft as part of an expanding multi-year partnership. *news.vt.edu*

Korea to test high-precision, real-time GPS service

South Korea will launch a test operation of a new GPS-based positioning service in October that works without an internet connection. The system, called the Gridded Virtual Reference Station (G-VRS), provides real-time location data with centimeter-level accuracy, making it useful in remote areas. GPS does not itself require an internet connection but devices typically use VRS systems that do rely on internet access improve location accuracy by creating a virtual network of reference points.

According to the National Geographic Information Institute, the G-VRS is designed to complement the current VRS system. It said the G-VRS system has proven accuracy similar to the existing VRS in actual environments. GNSS control points have been installed across the country, including four on Jeju

Island and one in Gageodo, an island off the southwestern coast. The state plans to install additional points on four islands, including Ulleungdo, about 120 kilometers off Korea's eastern coast, to operate 103 control points in total by the end of this year. *www.koreaherald.com*

Major Research Chair in Resilient GNSS navigation launched

CMC Electronics have partnered with École de Technologie Supérieure (ÉTS) to create the CMC Electronics Industrial Research Chair in Resilient GNSS Navigation. The five-year chair, valued at over $6 million, unites CMC's world-leading avionics expertise, led by Dr. John Studenny, internationally recognized GNSS navigation expert and standards contributor, with ÉTS's renowned LASSENA laboratory under Professor René Jr. Landry, a renowned expert in aerospace navigation and cybersecurity.

The Chair will tackle critical threats to aviation GNSS navigation, including jamming and spoofing. CMC and ETS will develop spoofing-resilient GNSS receivers capable of real-time detection, mitigation, and total recovery from spoofing attacks, setting a benchmark in aviation safety and integrity. *cmcelectronics.ca*

Maxar wins AIDC deal

Maxar Intelligence entered into a partnership with Taiwan's Aerospace Industrial Development Corporation (AIDC) to deploy it's Raptor software suite across Taiwan's unmanned aerial vehicle (UAV) industry. The software is designed to enable autonomous drones to navigate precisely and extract accurate ground coordinates in the absence of GPS. *www.satellitetoday.com*

Mass production of mosaic-G5 modules

Septentrio starts volume shipments of the recently announced mosaic-G5 modules. Measuring only 23 mm by 16 mm and weighing as little as 2.2 grams mosaic-G5 enables reliable positioning without performance compromises for commercial UAVs, robots, GIS devices and many other size and power-constrained industrial applications. *septentrio.com*

TDK launches DRIVE to unlock control-grade accuracy

TDK Corporation has launchesd Trusted Positioning DRIVE, an integrated GNSS and INS software solution, designed for advanced driver-assist systems (ADAS), robotic, and off-road vehicle platforms. It provides centimeter to decimeter level accuracy in real-world environments where GNSS alone is unreliable, providing customers the ability to scale and commercialize advanced control technologies economically.

Toyota and Australian scientists test GPS alternative

Toyota, the Royal Automobile Club of Queensland (RACQ), and Queensland's Department of Transport and Main Roads (TMR) have begun field tests of an Australian-developed navigation system designed to work in tunnels, buildings, and other places where conventional GPS does not work well.

The new Local Positioning System (LPS) is tested by attaching sensors to cars and e-scooters, then using custom software to gauge performance in "degraded road environments" such as tunnels and business districts where 'urban canyons' disrupt GPS signals.

It's the culmination of over two decades' worth of Queensland University of Technology (QUT) research work to build patented algorithms and hardware sensors, which have been tested for over two years with government transport bodies and the likes of Ford. *https://ia.acs.org.au*

CHC Navigation introduces visual-lidar GNSS RTK receiver

CHC Navigation (CHCNAV) has released the ViLi i100, its flagship visual-lidar GNSS RTK receiver. It offers consistent, centimeter-level accuracy, even where conventional GNSS receivers face limitations. Powered by the enhanced SFix 2.0 engine, the ViLi i100 maintains 5 cm accuracy while moving within a 20 m radius in GNSS-denied environments. It utilizes 860,000 points per second of laser data with SLAM-based algorithms to reconstruct its position without direct reliance on satellite signals. This capability allows for uninterrupted work in tunnels, under viaducts or within deep construction zones, providing a continuous workflow. *www.chcnav.com*

GPSIA urges Trump administration to tackle jamming and spoofing

The GPS Innovation Alliance (GPSIA) has released a set of recommendations that provides a roadmap for the Trump Administration to adopt a coordinated, whole-of-government approach to address the growing threat of harmful interference to the transportation industry resulting from jamming and spoofing of GPS, which risks public safety and impedes commerce. The recommendations call for executive branch agencies to:

- Accelerate the procurement and launch of modern GPS satellites and include anti-jamming and spoofing technology upgrades in ground systems. Prepare a program plan that ensures GPS is technologically more advanced than China's and Europe's GPS-like systems.
- Strengthen enforcement and coordination across the U.S. government to rapidly identify and respond to interference events and crack down on illegal sales and use of jamming devices.
- Streamline regulatory and certification processes to accelerate adoption of advanced technologies such as jam- and spoof-resistant antennas, modern GPS signals, and anti-spoofing signal authentication.
- Deter interference through public statements and diplomatic engagement, making clear the United States will not tolerate harmful jamming and spoofing outside conflict zones that risks public safety and impedes commerce. *www.gpsalliance.org*

In Coordinates

10 years before...

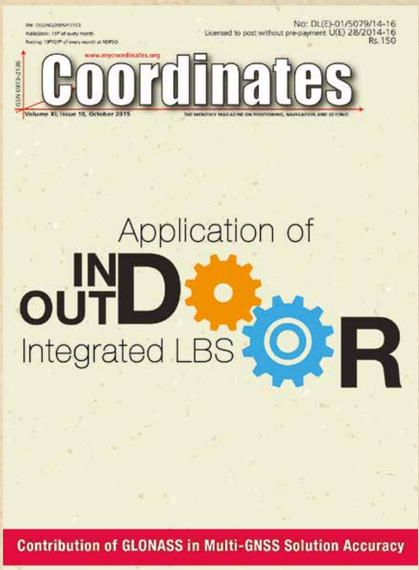

mycoordinates.org/vol-XI-issue-10-October-2015

Contribution of GLONASS in Multi-GNSS Solution Accuracy

Shreya Sarkar and Anindya Bose
Department of Physics, The University of Burdwan, Burdwan, West Bengal, India

Presented results here firstly show the advantages of Multi-GNSS (GPS+GLONASS) over single-mode operation providing improved solution accuracy in stand-alone, unaided operations. Presence of GLONASS, in general, supports to obtain better solution accuracy. The study also indicates that, when low number of GPS satellites are augmented with GLONASS, favourable improvement of solution accuracy is observed. Combinations of higher number of GPS satellites with increasing number of GLONASS though do not present similar benefit for improvement of solution accuracy.

The Comprehensive Cadastre

Dipl. Ing. ETH Jürg Kaufmann, Kaufmann Consulting, SLM Swiss Land Management Foundation, Rüdlingen, Switzerland

The Comprehensive Cadastre is therefore based on a data model, organized according to the legislation for the different legal land objects in a particular country or district.

While the traditional cadastre consists in general of one information layer representing the information about boundaries between different properties, in the Comprehensive Cadastre are added information layers representing the boundaries between land objects de¿ned by different legal topics, which exist in a jurisdiction.

Development and application of indoor/outdoor integrated location-based service

Ma Yang
China Siwei Surveying & Mapping Technology, Baishengcun, Zizhuyuan, Haidian, Beijing, China

Zhao Fangfang
Beijing NavInfo Science and Technology, Beijing Phoenix Place, Shuguang, Chaoyang, Beijing, China

Pang Zhe
Beijing NavInfo Science and Technology, Beijing Phoenix Place, Shuguang, Chaoyang, Beijing, China

By establishing complex indoor-and- outdoor integrative map models based on semantics and topology, we worked out standards and forms of data and production standard specifications of indoor- and-outdoor integrative maps. Some breakthroughs were also made in a few key technologies, such as integration of multi- source heterogeneous data, update of maps of crowdsourcing mode and visualization of 2D and 3D integrative indoor maps, with which we developed effective map production tools and 2D & 3D map engines.

Open source geo-information technology for making special purpose web-mapping application

Rouhollah Nasırzadeh Dızajı and Rahmi Nurhan Çelik
Istanbul Technical University (ITU), Department of Geomatic Engineering, Turkey

The result of the current work illustrates that it is possible to implement web mapping systems based solely on open-source software that are not only significantly more cost-effective than many commercial systems but also feature higher graphical quality, interactivity and flexibility.

New UltraCam Dragon 4.2 unveiled

Vexcel Imaging unveils the new UltraCam Dragon 4.2, the next evolution in hybrid aerial mapping technology. The new system features a significantly larger nadir and oblique image footprint, delivering a performance boost with 35% more flight line efficiency for faster data collection. Its powerful sensor suite combines two nadir cameras (RGB and NIR) and four high-resolution oblique RGB cameras (19,136 x 12,736 pixels each), with a 2.4 MHz RIEGL Waveform LiDAR scanner.

It delivers exceptional image quality by adhering to sound photogrammetric principles and leveraging Vexcel Imaging's True Pixel Processing (TPP) pipeline, which preserves all pixel information from capture to final product. At its core is Adaptive Motion Compensation (AMC), a proprietary software-based technology that automatically corrects for complex, multi-directional motion blur, ensuring sharp, accurate imagery across the entire project in a scene-aware manner.

UltraCam Merlin 5.0 debut in Australia

Latitude Spatial, Australia has become the first operator worldwide to integrate Vexcel Imaging's UltraCam Merlin 5.0 into active service. Though new in name, Latitude Spatial builds on decades of experience in aerial imaging and photogrammetry, including a long-standing operational history with UltraCam systems under the HyVista brand. *vexcel-imaging.com*

Trimble Comprehensive Data Collector Portfolio

Trimble has launched its comprehensive data collector portfolio, marking a new era of productivity and connectivity for geospatial and construction industries worldwide. This advanced suite of devices, including the Trimble TSC710 data collector, the Trimble TSC510 controller and the Trimble T110 tablet, is built for advanced functionality and effective integration across demanding field operations. When used with Trimble Connect®, a common data environment and collaboration platform, or Trimble WorksManager civil site management cloud software, users can take advantage of near real-time data exchange between the office and the jobsite to improve operations. *www.trimble.com*

Leica TS20 robotic total station

Leica Geosystems has launched the all-new Leica TS20 robotic total station. It accelerates fieldwork, simplifies daily work, streamlines repetitive tasks and avoids costly mistakes. It also incorporates insights gained directly from surveying practitioners to ensure it is specifically tailored to their real-world needs. A Neural Processing Unit (NPU) powers edge AI, enabling the Leica TS20 to optimise workflows autonomously, identify potential mistakes before they happen, and ensure reliable measurements while safeguarding data privacy. *leica-geosystems.com*

Leankon launches multi-band GNSS antenna

Leankon has introduced the LK1850301 Dipole FPC (Flexible PCB) GNSS antenna, engineered for seamless integration and high-performance positioning across various applications. It achieves an ultra-compact size of just 49 × 10 × 0.1 mm while supporting global multi-band GNSS. *www.leankon.com*

Telit Cinterion SE869eK5-DR GNSS module

Telit Cinterion, an end-to-end IoT solutions enabler, has announcesd the SE869eK5-DR, a dual-band, multi-constellation positioning receiver with untethered dead reckoning (UDR) built on the Airoha AG3335 chipset family. It features UDR which ensures reliable, continuous positioning even when satellite signals are lost due to jamming, interference or physical obstructions. *www.telit.com*

PlanetiQ wins largest commercial satellite weather data award

PlanetiQ has been awarded a $24.3 million contract from NOAA's National Environmental Satellite, Data, and Information Service (NESDIS). The award, issued under the Commercial Data Program's Radio Occultation Data Buy 2 (RODB-2), is NOAA's single largest commercial satellite weather data purchase. It will deliver 7,000 GNSS-RO profiles per day, including 500 enhanced high-signal-to-noise ratio (SNR) profiles as well as 2,500 low-latency Total Electron Content (TEC) tracks daily. *planetiq.com*

Safran's upgraded VersaSync GNSS master clock

Safran Electronics & Defense has released an enhanced version of VersaSync, its ruggedized GNSS master clock and network time server designed for defense applications. The system now offers improved frequency stability in harsh environmental conditions, including extreme temperatures, shock and vibration. Engineers have enhanced holdover performance for GNSS-denied missions and increased resistance to power supply transients to maintain timing continuity during platform power disruptions. *safran-navigation-timing.com*

u-blox launches ANN-MB3 compact triple-band antenna

u-blox has launched the ANN-MB3, its latest L1/L2/L5 triple-band RTK antenna. It is engineered to deliver validated high performance at reasonable cost, providing customers with a practical and scalable way to integrate high-precision positioning into their products. *www.u-blox.com*

BAE Systems and Forterra partnership

BAE Systems and Forterra are collaborating to rapidly prototype an autonomous Armored Multi-Purpose Vehicle (AMPV). This is the first industry partnership BAE Systems has established as part of the vehicle's capability kit series announced recently. The companies will create a highly survivable, self-driving AMPV prototype at speeds that rapidly outpace traditional development cycles, with plans to demonstrate the capability option and its technologies in 2026. *www.baesystems.com*

Ironstone Opal among best inventions of 2025

Q-CTRL has announced its software-ruggedized quantum navigation system's selection for TIME Best Inventions of 2025.Ironstone Opal, which has been field-validated in air, land, and maritime trials, provides a solution to GPS denial, which has become an increasing danger in conflict zones and recently threatened a plane carrying European Commission president Ursula von der Leyen. The system leverages quantum sensors, stabilized using software, to provide navigation that is immune to the kinds of interference plaguing commercial aviation, shipping, and defense operations. In airborne trials, Ironstone Opal enabled GPS-free navigation with an accuracy up to 111 times better than the best conventional GPS alternative, even under highly dynamic manoeuvres. It delivered GPS-like positioning accuracy down to just 4m over flights up to 700km long. *q-ctrl.com*

Eos Positioning to end four Arrow GNSS receivers in 2026

Beginning October 2, 2025, Eos will commence end-of-life planning for Arrow Lite®, Arrow 100®, Arrow 200®, Arrow Gold® receivers. Once existing inventory is exhausted, or March 31, 2026, whichever comes first, these models will officially be discontinued.

Eos remains committed to the customers and will continue to provide full support for these legacy products for a minimum of five years, in alignment with industry standards. Our technical support team and global distributor network will ensure our users may continue to rely on their devices with confidence and receive support when needed. *eos-gnss.com*

Juniper Systems partners with Point One Navigation

Juniper Systems, Inc. has announced a new strategic partnership with Point One Navigation. This collaboration will enable Juniper's Geode™ GNSS receivers to achieve seamless, centimeter-level accuracy through Point One's Polaris RTK corrections network. *pointonenav.com*

GEODNET launches GEO-MEASURE

GEODNET has launched GEO-MEASURE, a survey-grade GNSS rover that delivers centimeter-level accuracy at a consumer-accessible price. It integrates robust hardware, a dedicated mobile app, and a preloaded RTK corrections service into a single turnkey package. It is engineered for professional reliability with quad-frequency support across GPS, GLONASS, Galileo, and BeiDou, 1,040 tracking channels for resilience under canopy or in urban environments, and a rugged, waterproof housing built for daily use. *geodnet.com*

Mayflower expands anti-jam portfolio

Mayflower Communications Company, Inc has been granted two pivotal U.S. patents—US 11,262,457 and US 12,235,365—that significantly advance its GNSS anti-jam capabilities. These patents expand Mayflower's proprietary technology into Signals of Opportunity (SoOP), enabling interference suppression across both Iridium and GNSS frequency bands. GPS remains a cornerstone of PNT for both military and commercial platforms. However, its vulnerability to intentional and unintentional jamming and spoofing has underscored the need for more resilient PNT solutions. *www.mayflowercom.com*

Drone combines LiDAR, Photogrammetry, RTX GNSS, and Starlink

The ORKID 260 vertical take-off and landing (VTOL) integrated drone combines LiDAR, photogrammetry, GNSS, and Starlink satellite connectivity onboard, allowing all systems to operate simultaneously. It features the YellowScan Surveyor Ultra LiDAR, Phase One P5 camera, Trimble Applanix APX-RTX GNSS with real-time corrections, and native Starlink SATCOM integration. It is designed to perform all data collection functions in one mission, providing seamless calibration, synchronization, and data management. *dronelife.com*

NSG Geospatial Services launches "NeoMaps"

NSG Geospatial Services has launched "NeoMaps". This launch underscores the company's role in supporting the Kingdom's efforts to develop geospatial capabilities and enhance digital sovereignty in this vital sector, contributing to Saudi Arabia's leading position in the geospatial economy at both regional and global levels. The platform is distinguished by its ability to integrate diverse data resources from multiple sources and to enable users to perform core GIS functions, such as exploring map content online, changing base maps, adding data layers, and customizing their styles.

SUBSCRIPTION FORM

YES! I want my Coordinates

I would like to subscribe for (tick one)

☐ 1 year	☐ 2 years	☐ 3 years
12 issues	24 issues	36 issues
Rs.1800/US$140	Rs.3400/US$200	Rs.4900/US$300
*		SUPER saver

First name ....

Last name ....

Designation ....

Organization ....

Address ....

....

City .... Pincode ....

State .... Country ....

Phone ....

Fax ....

Email ....

I enclose cheque no. ....

drawn on ....

date .... towards subscription

charges for Coordinates magazine

in favour of **'Coordinates Media Pvt. Ltd.'**

Sign .... Date ....

Mail this form with payment to:

Coordinates
A 002, Mansara Apartments
C 9, Vasundhara Enclave
Delhi 110 096, India.

If you'd like an invoice before sending your payment, you may either send us this completed subscription form or send us a request for an invoice at iwant@mycoordinates.org

* Postage and handling charges extra.

MARK YOUR CALENDAR

November 2025

Canada's National Geomatics Expo 2025
3 - 5 November
Calgary, Canada
https://gogeomaticsexpo.com

13th International FIG Workshop on the Land Administration Domain Model & 3D Land Administration
3 - 5 November 2025
Florianópolis, Santa Catarina, Brazil
https://gdmc.nl

Trimble Dimensions
10 - 12, November 2025
Las Vegas, USA
www.trimble.com

3rd International Workshop on Evaluation and BENCHmarking of Sensors, Systems and GEOspatial Data in Photogrammetry and Remote Sensing (GEOBENCH)
20 - 21 November 2025
Wroclaw, Poland
https://geobench.fbk.eu

Geo World 2025
24 - 27 November
Dubai, UAE
www.geoworldevent.com

February 2026

Geo Week
16 - 18, February 2026
Denver, CO, USA
www.geo-week.com

DGI 2026
23 -25 February
The Queen Elizabeth II Centre, London
https://dgi.wbresearch.com

March 2026

Munich Navigation Satellite Summit
25 - 27 March 2026
Munich, Germany
www.munich-satellite-navigation-summit.org

Geo Connect Asia 2026
31st March - 01st April
Singapore
www.geoconnectasia.com

April 2026

European Navigation Conference 2026
28 – 30 April 2026
Vienna, Austria
https://enc-series.org

May 2026

GISTAM 2026
21-23 May
Benidorm, Spain
https://gistam.scitevents.org

FIG 2026
24 - 29 May
Cape Town, South Africa
https://fig2026.org

GeoCue introduces Immersive Image Explorer

GeoCue has released the Immersive Image Explorer in LP360. It fuses captured imagery with LiDAR point clouds, enabling professionals to virtually "walk through" their scanned environments inside LP360. Whether collected from aerial, mobile, or handheld TrueView systems, imagery can now be overlaid directly behind point clouds for a richer, more intuitive exploration experience. *www.geocue.com*

Satellite to study space radiation and climate

SFL Missions Inc. has been awarded a contract by the University of Alberta for development of the RADICALS small satellite to study the transport of space radiation into Earth's atmosphere and its impact on climate. The RADiation Impacts on Climate and Atmospheric Loss Satellite (RADICALS) mission is being designed by a consortium of Canadian Universities and SFL Missions, led by the University of Alberta, and funded by the Canada Foundation for Innovation, the Government of Alberta, and the Canadian Space Agency.

Built on the space-proven SFL DEFIANT bus, RADICALS will leverage SFL's flexibility in attitude control approaches and require the spacecraft to spin end-over-end as it travels in a near-polar orbit around Earth. This will enable its suite of multiple instruments to collect continuous measurements of the full angular distribution of the space radiation which rains down into the Earth's atmosphere, these 360-degree directional measurements being essential for quantifying the energy input with unprecedented accuracy.

RADICALS will carry three multi-sensor instrument suites – an X-ray Imager (XRI), High Energy Particle Telescope (HEPT), and Magnetometers (MAGS), with a total of 11 sensors. *sflmissions.com*